

The Schwarzian Theory - A Wilson Line Perspective

Andreas Blommaert^{*}, Thomas G. Mertens[†] and Henri Verschelde[‡]

*Department of Physics and Astronomy
Ghent University, Krijgslaan, 281-S9, 9000 Gent, Belgium*

Abstract

We provide a holographic perspective on correlation functions in Schwarzian quantum mechanics, as boundary-anchored Wilson line correlators in Jackiw-Teitelboim gravity. We first study compact groups and identify the diagrammatic representation of bilocal correlators of the particle-on-a-group model as Wilson line correlators in its 2d holographic BF description. We generalize to the Hamiltonian reduction of $SL(2, \mathbb{R})$ and derive the Schwarzian correlation functions. Out-of-time ordered correlators are determined by crossing Wilson lines, giving a $6j$ -symbol, in agreement with 2d CFT results.

May 18, 2022

^{*}andreas.blommaert@ugent.be

[†]thomas.mertens@ugent.be

[‡]henri.verschelde@ugent.be

Contents

1	Introduction	2
2	Particle-on-a-group Theory	3
2.1	Correlation Functions in BF	5
2.1.1	Open Channel Description	5
2.1.2	Wilson Lines	8
2.2	Holography in BF	10
2.3	Diagrammatic Expansion	12
3	Interlude: Non-Compact Groups	14
4	Schwarzian Theory	15
4.1	Liouville as Constrained WZW	16
4.2	Schwarzian as Constrained Particle-on-a-group	17
4.3	Correlation Functions in Constrained BF	18
4.3.1	Open Channel Description	18
4.3.2	Wilson Lines	21
4.4	Holography in Constrained BF	23
4.5	Diagrammatic Expansion	25
5	Concluding Remarks	27
A	Knots in BF	28
A.1	Punctures	29
A.2	Diagrammatic Rules	33
A.3	Wilson Loop Crossings	33
B	Some Elementary Properties of Representation Matrices	34
C	WZW and Particle-on-a-group	35
C.1	Non-Chiral WZW	35
C.2	Coadjoint Orbit	36
C.3	Branes	38
D	Correlation Functions in Particle-on-a-group	39
E	Representation Theory of $SL(2, \mathbb{R})$ in the Parabolic Basis	41
E.1	Parabolic Basis	41
E.2	Constrained $SL(2, \mathbb{R})$ basis	44
E.3	From the $SL(2, \mathbb{R})$ Casimir to the minisuperspace Liouville Hamiltonian	46
E.4	6j-symbol	46
F	Representation Theory of $SL(n, \mathbb{R})$ in the Parabolic Basis	47

1 Introduction

Exactly solvable quantum systems that exhibit holographic features are very scarce. Therefore every example one finds should be thoroughly understood. The past few years, it became clear that one such example is the Sachdev-Ye-Kitaev (SYK) model (and its relatives) [1–12]. These models describe N Majorana fermions interacting through a random all-to-all 4-point interaction. The model is diagrammatically tractable at large N , and many features are understood by now. A very interesting regime is that of strong coupling, where the model is effectively described by Schwarzian quantum mechanics:

$$S = -C \int dt \{f, t\}, \quad (1.1)$$

where $\{f, t\} = \frac{f'''}{f'} - \frac{3}{2} \frac{f''^2}{f'^2}$ denotes the Schwarzian derivative of f . It was immediately realized that a 2d dilaton gravity theory in AdS_2 - the Jackiw-Teitelboim (JT) model - has dynamics described by precisely this same Schwarzian action [13–22], such that the Schwarzian theory can be used to study a 2d quantum gravity. Motivated by this, using the structural link of Schwarzian quantum mechanics with 2d Virasoro CFT, the quantum dynamics of the Schwarzian theory was discussed in [23, 24], with the link with the semi-classical regime in JT gravity explicitly uncovered in [25]. Several avenues towards Schwarzian correlation functions of bilocal operator insertions exist by now: the 2d Liouville perspective was explored in [23, 24], a 1d Liouville approach was analyzed in [26, 27], and a particle on H_2^+ in an infinite (imaginary) magnetic field is explored in [28]. Whereas each approach has its own value, this does leave open the question of whether these results can be found directly from Jackiw-Teitelboim gravity. In particular, we would like to know what is the bulk JT gravity interpretation of the bilocal Schwarzian operators. We will answer this question using the topological BF formulation of JT gravity. The relation of

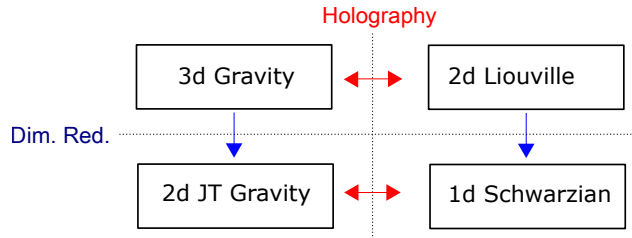


Figure 1. Relation through holography and dimensional reduction of 3d $\Lambda < 0$ gravity, 2d JT gravity, 2d Liouville CFT and 1d Schwarzian QM.

the Schwarzian with Liouville and JT gravity is depicted in Figure 1.

It was realized soon after in [24, 29], that the above gravitational story is only the irrational case (in a 2d CFT sense) of a more generic story that includes Wess-Zumino-Witten (WZW) CFT and Chern-Simons (CS) / BF bulk theories. The analogue of the Schwarzian model is played by the 1d particle-on-a-group theory (Figure 2). This model also appears in SYK models with internal symmetries [30–34], as a building block of the supersymmetric theories [35], and in higher spin generalizations [36]. Correlation functions of the 1d

particle-on-a-group theory were determined using the identification of particle-on-a-group as the dimensional reduction at $k \rightarrow +\infty$ of WZW [24]. This is the rightmost track of Figure 2. In the first part of this work, we will arrive at these same correlation functions using

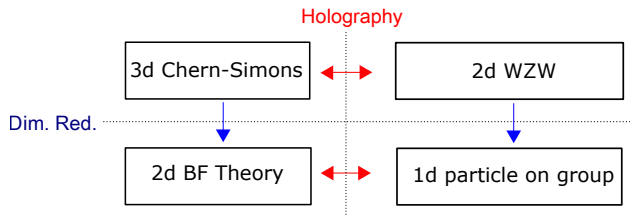


Figure 2. The 3d Chern-Simons / 2d WZW holographic relation, which dimensionally reduces to the 2d BF / 1d particle-on-a-group holography.

holography of the 2d BF theory (using the bottom track in Figure 2). This will provide a complementary perspective on the previous derivations, and in particular on the out-of-time ordered (OTO) correlators. The results presented here for BF theory were already anticipated in [37], where we investigated the particle-on-a-group model as describing the edge dynamics of 2d Yang-Mills on a disk.

It is well-known that AdS_3 gravity / Liouville are constrained versions of respectively $\text{SL}(2, \mathbb{R})$ CS / WZW [38–40], generalizing the well-known compact story [41–43]. In this work, we will exploit the dimensional reduction of this gauge theory perspective on AdS_3 gravity and discuss JT gravity / Schwarzian as a constrained version of $\text{SL}(2, \mathbb{R})$ BF / particle-on-a-group. The result is a bulk JT derivation of Schwarzian correlators.

In section 2 we discuss the bulk BF interpretation of correlators in particle-on-a-group. After a brief discussion on non-compact generalizations in section 3, we generalize to the Schwarzian / Liouville theories in section 4. We resort to the conventional Hamiltonian reduction of $\text{SL}(2, \mathbb{R})$ to find out how Schwarzian correlators are related to a constrained $\text{SL}(2, \mathbb{R})$ BF theory. We end in section 5 with some possibilities to pursue in the future, in particular we make a short detour to higher spin Schwarzian systems, focusing on the $\text{SL}(n, \mathbb{R})$ Hamiltonian reduction. In order to make the presentation self-contained, the appendices contain some review material on what we need of $\text{SL}(2, \mathbb{R})$ representation theory and the higher spin generalization.

Note Added

A related approach is being developed in [44].

2 Particle-on-a-group Theory

We consider in this section correlators of boundary-anchored Wilson lines in BF theory with specific boundary conditions and prove a 1:1 relation with bilocal correlators in the 1d particle on a group theory.

Dimensional reduction of 3d Chern-Simons with a boundary results in 2d BF theory [24] (using the left track in figure 2):

$$S[\chi, A] = \int \text{Tr}(\chi F) + \frac{1}{2} \int d\tau \text{Tr}(\chi A_\tau). \quad (2.1)$$

Introducing a 1d metric $\gamma_{\tau\tau}$ along the boundary curve, we impose the boundary condition $\chi|_{\text{bdy}} = C\sqrt{\gamma_{\tau\tau}}A_\tau|_{\text{bdy}}$ for some fixed constant C . The bulk is topological, but this is broken by the boundary condition, and one finds the energy-momentum tensor:

$$T_{\tau\tau}(\tau) \equiv \frac{2}{\sqrt{\gamma}} \frac{\delta S}{\delta \gamma^{\tau\tau}} = \frac{1}{2C} \text{Tr}(\chi^2) = L_{\text{bdy}}, \quad (2.2)$$

setting $\gamma_{\tau\tau} = 1$ in the end. Hence the choice of boundary term is crucial. This is manifest when choosing alternatively e.g. $A_\tau|_{\text{bdy}} = 0$: this puts $H(\tau) = 0$ and destroys the boundary dynamics. In that case, we are left with the completely topological theory

$$S[\chi, A] = \int \text{Tr}(\chi F). \quad (2.3)$$

Notice that this is just the $e \rightarrow 0$ limit of 2d Yang-Mills theory with boundary conditions $A_\tau|_{\text{bdy}} = 0$ [45, 46].⁴ Structurally, the theory (2.1) is then very similar to 2d Yang-Mills (YM) theory, a feature which will become more apparent below. We explore this completely topological BF-theory and its observables in Appendix A applying traditional techniques. The observables in Chern-Simons are Wilson lines and this continues to hold after dimensional reduction to BF. As in CS, observables of BF split into topological bulk observables (knots discussed in Appendix A), and dynamical observables associated with boundary dynamics: boundary-anchored Wilson lines. Here we will only be interested in the latter. In particular we will restrict ourselves to Wilson lines with both endpoints on the boundary: networks of Wilson lines are left for future work.⁵

We will mainly be interested in the thermal theory (2.1) defined on a disk. In order to compute the partition function and the correlation functions, we will employ a slicing of the theory in intervals (instead of the usual circles employed in e.g. [45–48]). We will utilize several different descriptions of the same amplitude, as in Figure 3. The left Figure describes an open channel slicing with identity boundary states that we will explore in 2.1.1. The middle Figure is, due to the topological invariance of the model manifestly the same, and is an instructive slicing to link with the brane description of [23, 24]. The right Figure describes a boundary-intrinsic particle-on-a-group perspective that we will discuss in section 2.2.

⁴The equivalence is proven in the path integral by integrating out χ in the action

$$S[\chi, A] = \frac{e}{2} \int d^2x \sqrt{g} \text{Tr}(\chi^2) + \int \text{Tr}(\chi F), \quad (2.4)$$

which becomes (2.3) in the limit $e \rightarrow 0$.

⁵Such networks of Wilson lines have natural holographic duals in the particle-on-group and Schwarzian models, though they are not the bilocal boundary operators we are interested in here.

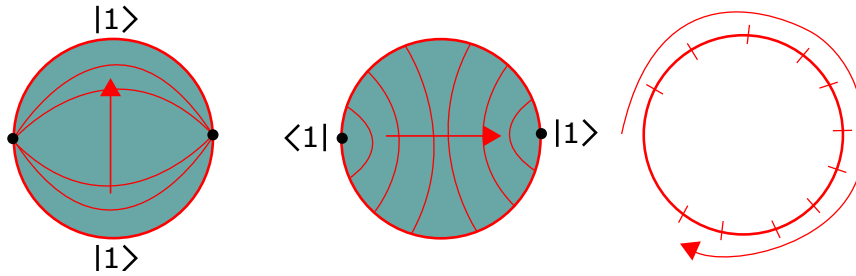


Figure 3. Left: disk amplitude in the open channel. Middle: disk amplitude in the crossed channel. Right: Boundary circle with evolution along the circle.

2.1 Correlation Functions in BF

Let us now calculate boundary anchored Wilson line amplitudes in 2d BF theory, and 2d YM, with a boundary. This is an extension of the known correlators [45–48].

2.1.1 Open Channel Description

Though 2d YM and BF are distinct theories (the first is quasi-topological and the second fully topological), quantizing them on a manifold with boundaries requires the same techniques. This is due to the lack of propagating degrees of freedom in two dimensions and the fact that both theories have an identical Hilbert space structure, determined by the Peter-Weyl theorem; when quantizing the theory on a circle, the Hilbert space consists of the irreps whose normalized wavefunctions are the characters $\chi_R(g) = \langle g|R \rangle = \text{Tr } R(g)$.

For the purpose of calculating boundary-anchored Wilson lines, we are interested instead in quantizing the theory on an interval: the Peter-Weyl theorem now states that the Hilbert space is spanned by all matrix elements of the unitary irreducible representations of the group. The same logic was used to write 2d Yang-Mills on a sphere as an open string theory in [49]. The normalized wavefunctions are given by:

$$\langle g|R, ab \rangle = \sqrt{\dim R} R_{ab}(g), \quad (2.5)$$

where $R_{ab}(g) = \langle a|g|b \rangle$ is the matrix element in the representation R . Two conjugate bases for the Hilbert space of BF theory (or particle-on-a-group) are hence $|R, ab \rangle$ and the group elements $|g \rangle$. For example, for $U(1)$ these would be the discretized charges $|q \rangle$ or the angular coordinate $|\phi \rangle$ respectively. The appropriate normalization of the wavefunctions is deduced from the grand orthogonality theorem:⁶

$$\int dg R_{ab}(g) R'_{cd}(g^{-1}) = \frac{\delta_{RR'}}{\dim R} \delta_{ad} \delta_{bc}, \quad (2.6)$$

and orthonormality of the wavefunctions. Note that (2.6) is fixed by the normalization $R_{ab}(\mathbf{1}) = \delta_{ab}$ which in turn is enforced by the defining property of representation matrices $R_{ab}(\mathbf{1}) R_{bc}(\mathbf{1}) = R_{ac}(\mathbf{1})$.

⁶We gather some relevant equations in Appendix B.

Both for YM and BF, the Hamiltonian reduces to the Casimir of the algebra, hence the basis states $|R, ab\rangle$ are also eigenstates of the Hamiltonian. Specifically, for BF the boundary-supported Hamiltonian propagation factor evaluated in a state $|R, ab\rangle$ is:

$$TH(R) = L \frac{\mathcal{C}_R}{C}, \quad (2.7)$$

with L the length of the boundary segment propagated over, and \mathcal{C}_R the Casimir in the irrep R . Note that only the physical boundaries of the 2d manifold come with a boundary Hamiltonian contribution,⁷ and that the Hamiltonian is independent of the labels a and b . Likewise, for 2d YM with action

$$S[A] = \frac{1}{2e} \int d^2x \sqrt{g} \text{Tr} F^2, \quad (2.8)$$

the Hamiltonian propagation factor scales with the area A and the coupling e :

$$TH(R) = eAC_R. \quad (2.9)$$

Consider now a disk-shaped surface and divide the circular boundary into two intervals. Associate a state $|g\rangle$ with the first interval and a state $|h\rangle$ with the second. The situation is shown on the left of Figure 4. The partition function of this disk is:

$$Z_{\text{disk}}(g, h) = \langle g | e^{-TH} | h \rangle. \quad (2.10)$$

The states $|g\rangle$ and $|h\rangle$ in (2.10) can be viewed as *boundary states*, that can be expanded in the representation basis using (2.5):

$$|g\rangle = \sum_{R,m,n} \sqrt{\dim R} R_{mn}(g) |R, mn\rangle. \quad (2.11)$$

Let us now demonstrate the correctness of this open channel perspective provided in (2.10) by rederiving the known 2d YM results [45, 46] from it. Inserting a completeness relation in (2.10), we obtain:

$$Z_{\text{disk}}(g, h) = \sum_{R,a,b} \langle g | R, a, b \rangle \langle R, a, b | h \rangle e^{-TH(R)} = \sum_{R,a,b} \dim R R_{ab}(g) R_{ba}(h^{-1}) e^{-TH(R)}. \quad (2.12)$$

Denoting the holonomy $U = g \cdot h^{-1}$ along the entire boundary of the disk and using $\chi_R(U) = \text{Tr} R(U)$ this matches with the calculation of the disk partition function from the closed channel [45, 46]:

$$Z_{\text{disk}}(U) = \sum_R \dim R \chi_R(U) e^{-TH}. \quad (2.13)$$

Alternatively, using the definition of irrep matrices and splitting g as $g = g_A \cdot g_B \cdot g_C$ we can rewrite the disk amplitude as a rectangle amplitude as in the right of Figure 4:

$$Z_{\text{rect}}(h, g_A, g_B, g_C) = \sum_{R,a,b,x,y} \dim R R_{ax}(g_A) R_{xy}(g_B) R_{yb}(g_C) R_{ba}(h^{-1}) e^{-TH(R)}. \quad (2.14)$$

⁷Gluing different patches together results in a net cancellation of the Hamiltonian density on the gluing curve, such that gluing is consistent with the concept of a boundary Hamiltonian.

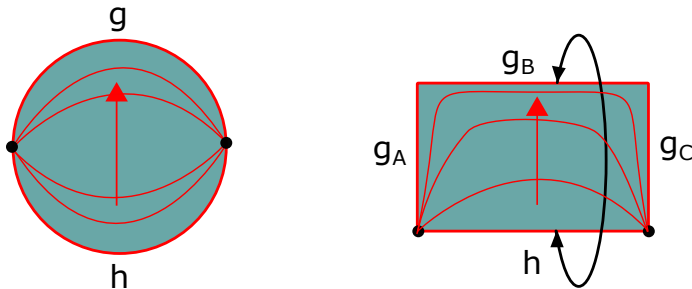


Figure 4. The disk amplitude in the open channel (left). Hilbert space slicings are denoted in red. Deforming the amplitude (either preserving the area (YM), or the boundary length (BF)) into a rectangle (right), and identifying the upper and lower boundaries, one arrives at the fundamental cylinder amplitude.

This can be glued into a cylinder by gluing along the boundaries and using (2.6) as

$$Z_{\text{cyl}}(g_A, g_C) = \int dh dg_B \delta(h - g_B) Z_{\text{rect}}(h, g_A, g_B, g_C) = \sum_{R,a,b} \chi_R(g_A) \chi_R(g_C) e^{-TH(R)}, \quad (2.15)$$

Again this matches with the closed channel calculation of the annulus. Reproducing the disk and the annulus proves by induction (gluing) that the open-channel calculations result in the correct partition function on a generic 2d manifold [45–48], and thus confirms the validity of our open-channel approach. Physical boundary segments of 2d YM or BF are characterized by $g = h = \mathbf{1}$ [37]. The disk partition function becomes:

$$Z_{\text{disk}} = \sum_{R,m} \dim R e^{-\beta \frac{c_R}{C}} = \sum_R (\dim R)^2 e^{-\beta \frac{c_R}{C}}, \quad (2.16)$$

indeed equal to the partition function of a particle on a group manifold [50, 51].

It is useful to look at these same calculations from the perspective of yet another Hilbert space slicing, this to make contact with the computations performed in [23, 24], where particle-on-a-group correlators were obtained by dimensionally reducing WZW (see Appendix C). Consider the “point-defect” slicing of Figure 5 left. The calculation of the disk amplitude is precisely the same as the above. Now however, the boundary states are associated with point-like defects. Setting again $g = h = \mathbf{1}$ identifies these defects as the dimensional reduction of the vacuum brane inserted in WZW, which is also characterized by $g = h = \mathbf{1}$.⁸ The thermal boundary circle of Figure 5 denotes the doubled space ob-

⁸The boundary state $|\mathbf{1}\rangle$ is also closely related to the so-called Ω -state in 2d YM, introduced by Gross and Taylor in [52], and interpreted in [49] as an entanglement brane. Whereas the latter is a state in the closed (chiral) Hilbert space (i.e. a class function), and is expanded in a basis of irreps as

$$|\Omega\rangle = \sum_R \dim R |R\rangle, \quad (2.17)$$

the former resides in the open Hilbert space, and is expanded as

$$|\mathbf{1}\rangle = \sum_{R,m} \sqrt{\dim R} |R, mm\rangle. \quad (2.18)$$

tained after performing the doubling trick; before dimensional reduction this was the torus on which the chiral (effect of the branes) WZW lives. This same observation will turn out to hold for the JT gravity / Schwarzian: the boundary defects are the dimensional reduction of ZZ-branes $\phi \rightarrow \infty$.

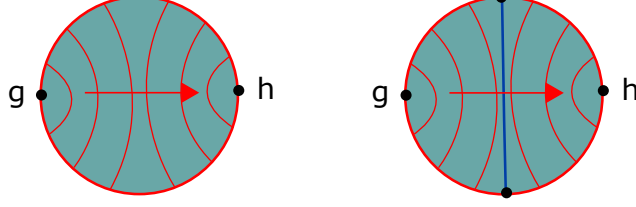


Figure 5. Left: Hilbert space slicing in the point-defect channel, representing propagation between pointlike defects. Right: Amplitude with a Wilson line inserted.

2.1.2 Wilson Lines

Armed with this open-channel formalism we can now directly calculate generic correlators of boundary-anchored Wilson lines in 2d YM and BF, in the same manner as was done in the past for closed Wilson loops in 2d YM. Basically the only tools we need are the disk amplitudes (2.12), the identification of a Wilson line segment in irrep R with starting point and endpoint labeled by m respectively n evaluated on group element g as $R_{mn}(g)$, and the integral over three representation matrices:

$$\int dg R_{1,m_1 n_1}(g) R_{2,m_2 n_2}(g) R_{3,m_3 n_3}(g) = \begin{pmatrix} R_1 & R_2 & R_3 \\ m_1 & m_2 & m_3 \end{pmatrix} \begin{pmatrix} R_1 & R_2 & R_3 \\ n_1 & n_2 & n_3 \end{pmatrix}. \quad (2.19)$$

As an instructive example, consider the diagram with a single Wilson line in the bulk (Figure 6 left). To compute the amplitude, we separate the disk in two halves, and apply

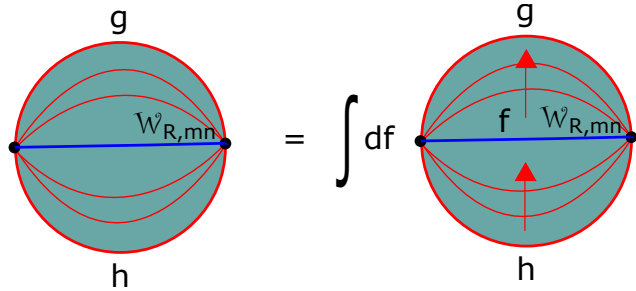


Figure 6. Left: Disk with a single Wilson line inserted. Red lines are Hilbert space slicings. Right: Computation done by splitting the disk into two semidisks with the Wilson line in the middle.

our previous computation to both sides:

$$\langle g | e^{-TH} \mathcal{W}_{R,mn} | h \rangle = \int df \langle g | e^{-T_1 H} | f \rangle \mathcal{W}_{R,mn}(f) \langle f | e^{-T_2 H} | h \rangle. \quad (2.20)$$

The gluing integral over the intermediate group variable f is then computable by (2.19). In formulas:

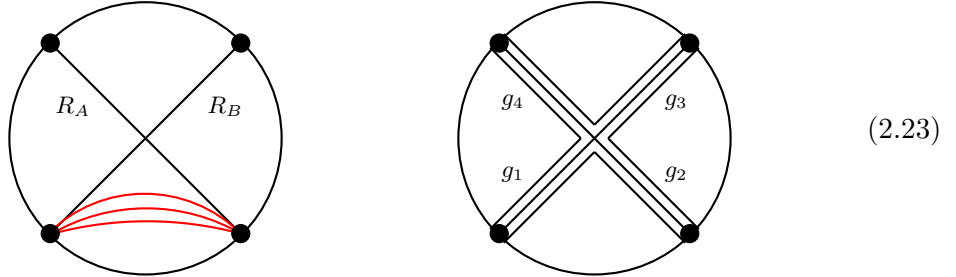
$$\begin{aligned}
& \sum_{R_i, m_i, n_i} \langle g | R_{1, m_1 n_1} \rangle e^{-T_1 \frac{C_{R_1}}{C}} \int df \langle R_{1, m_1 n_1} | f \rangle R_{mn}(f) \langle f | R_{2, m_2 n_2} \rangle e^{-T_2 \frac{C_{R_2}}{C}} \langle R_{2, m_2 n_2} | h \rangle \\
&= \sum_{R_i, m_i, n_i} \dim R_1 \dim R_2 R_{1, m_1 n_1}(g) R_{2, m_2 n_2}(h^{-1}) e^{-T_1 \frac{C_{R_1}}{C}} e^{-T_2 \frac{C_{R_2}}{C}} \\
&\quad \times \int df R_{1, m_1 n_1}(f^{-1}) R_{mn}(f) R_{2, m_2 n_2}(f). \tag{2.21}
\end{aligned}$$

Setting again $g = h = \mathbf{1}$, one recovers the particle-on-a-group result [24]:

$$\left\langle \mathcal{O}_{R, mn}(\tau_1, \tau_2) \right\rangle = \delta_{mn} \sum_{R_i, m_1, m_2} \dim R_1 \dim R_2 e^{-T_1 C_{R_1}} e^{-T_2 C_{R_2}} \begin{pmatrix} R_1 & R & R_2 \\ m_1 & m & m_2 \end{pmatrix}^2. \tag{2.22}$$

Again, it is instructive to rephrase this amplitude in the point-defect channel (Figure 5 right). The Wilson line operator has one end on each side of the boundary, in line with the general idea that local non-chiral CFT operators map to bilocal operators in particle-on-a-group on account of the doubling that takes the non-chiral CFT between branes to the chiral CFT.

A bulk crossing of Wilson lines can be dealt with using methods already developed in the 2d YM context [46].



On the left, we have drawn some slices of the open channel Hilbert space in the bottom wedge. Zooming on this bottom wedge only (Figure 7), we can write the wavefunction on the top edges of this wedge by decomposing the representation matrices as

$$R_{m\bar{m}}(g_1 \cdot g_2) = \sum_n R_{mn}(g_1) R_{n\bar{m}}(g_2). \tag{2.24}$$

This is repeated for each wedge. Combining the resulting representation matrices with the $R_{mn}(g)$ associated to the Wilson line itself, one needs to integrate products of three representation matrices on a single group element $g_i, i = 1 \dots 4$, as in (2.19). This procedure can be suggestively written graphically by explicitly drawing lines associated to the R_{mn} within each wedge, and artificially separating the wedge contributions from the Wilson line contributions, as in the right of (2.23). These group integrals lead to four $3j$ -symbols associated to the four outer vertices (the four big black dots in (2.23)), and four $3j$ -symbols

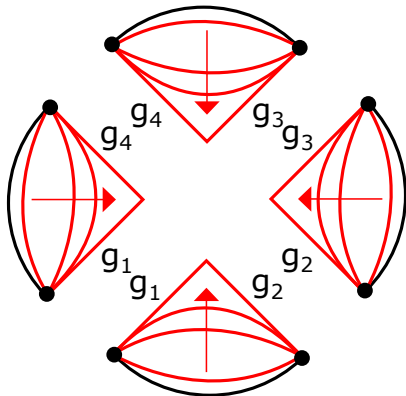


Figure 7. Hilbert space slicing within each of the wedges. We are interested in the Hilbert space description on the final slice, consisting of two connected straight lines.

associated to the internal vertex. The latter still contains a sum over m -labels, resulting in a $6j$ -symbol:

$$\left\{ \begin{matrix} R_B & R_1 & R_4 \\ R_A & R_3 & R_2 \end{matrix} \right\} = \sum_{m_i, m_A, m_B} \begin{pmatrix} R_1 & R_2 & R_A \\ m_1 & m_2 & m_A \end{pmatrix} \begin{pmatrix} R_2 & R_3 & R_B \\ m_2 & m_3 & m_B \end{pmatrix} \begin{pmatrix} R_3 & R_4 & R_A \\ m_3 & m_4 & m_A \end{pmatrix} \begin{pmatrix} R_4 & R_1 & R_B \\ m_4 & m_1 & m_B \end{pmatrix}, \quad (2.25)$$

for each crossing of Wilson lines.

At the beginning of this section 2, we commented that Wilson lines can be freely deformed: moving Wilson lines through each other, leaves the amplitudes unchanged. Armed with the specific expressions, we check this explicitly in Appendix A.3.

2.2 Holography in BF

In this section, we will make the link with the particle-on-a-group model more explicit, and provide another derivation of the correlators directly in this language. Starting with (2.1), path-integrating over the bulk χ forces $F = 0$ and hence renders A flat: $A = -dgg^{-1}$. This holds even when Wilson line operators are inserted into the path integral. The Hamiltonian of the theory lives on the boundary and is completely determined by the *choice* of boundary conditions. Choosing $\chi|_{\text{bdy}} = CA_\tau|_{\text{bdy}}$, the BF theory reduces to a boundary theory with particle on group action [24]:

$$S[g] = \frac{C}{2} \int d\tau \text{Tr}(g^{-1} \partial_\tau g g^{-1} \partial_\tau g), \quad (2.26)$$

with coupling C determined by the choice of boundary conditions and the path integral over $g \in LG/G$, the right coset of the loop group of G .⁹ As the theory fully reduces to

⁹An alternative way to obtain the particle on group action from BF theory is to add a term to the BF action that enforces a specific boundary condition:

$$S[\chi, A] = \int \text{Tr}(\chi F) + \frac{1}{2} \int d\tau \text{Tr}(\chi A_\tau) + \frac{1}{4C} \int d\tau \sqrt{h} \text{Tr}(\chi^2). \quad (2.27)$$

Path integrating over χ entirely results again in (2.26).

the boundary particle-on-a-group, this provides an alternative and direct explanation of the Hilbert space structure as the Peter-Weyl decomposition of an arbitrary function in $L^2(G)$, the group element g being just the dynamical variable of the boundary quantum mechanical model.

The matrix elements of a Wilson line from boundary point τ_i to τ_f in representation R are:

$$\mathcal{W}_{R,mn}(\tau_i, \tau_f) = \mathcal{P} \exp \left\{ - \int_{\tau_i}^{\tau_f} R(A) \right\}_{mn}. \quad (2.28)$$

The identification of correlators of boundary-anchored Wilson lines in BF as correlators of bilocals in particle on group can be proven by observing that upon integrating out the bulk χ of BF theory which renders A flat, the path-ordered exponential (2.28) reduces to a bilocal operator:

$$\boxed{\mathcal{W}_{R,mn}(\tau_i, \tau_f) = R_{mn}(g(\tau_f)g^{-1}(\tau_i)) = \mathcal{O}_{R,mn}(\tau_i, \tau_f)}. \quad (2.29)$$

These bilocals are precisely the operators whose particle-on-a-group correlators were calculated from WZW correlators in [24].

We can use this dictionary to directly compute correlation functions of the particle-on-a-group theory, without resorting to the holographic bulk and Wilson line description. Writing two bilocal operators as:

$$\begin{aligned} \mathcal{W}_{R_A, m_A \bar{m}_A} &= R_A(g_2)_{m_A \alpha} R_A(g_1^{-1})_{\alpha \bar{m}_A}, \\ \mathcal{W}_{R_B, m_B \bar{m}_B} &= R_B(g_4)_{m_B \beta} R_B(g_3^{-1})_{\beta \bar{m}_B}, \end{aligned} \quad (2.30)$$

the time-ordered four-point correlator is computed in the particle-on-a-group model as the thermal trace:

$$\text{Tr} \left[e^{-\beta H} R_B(\hat{g}_4)_{m_B \beta} R_B(\hat{g}_3^{-1})_{\beta \bar{m}_B} R_A(\hat{g}_2)_{m_A \alpha} R_A(\hat{g}_1^{-1})_{\alpha \bar{m}_A} \right], \quad (2.31)$$

with H the Hamiltonian associated to (2.26). The computation itself involves inserting complete sets of states and is deferred to Appendix D. Instead taking crossing bilocals as

$$\begin{aligned} \mathcal{W}_{R_A, m_A \bar{m}_A} &= R_A(g_3)_{m_A \alpha} R_A(g_1^{-1})_{\alpha \bar{m}_A}, \\ \mathcal{W}_{R_B, m_B \bar{m}_B} &= R_B(g_4)_{m_B \beta} R_B(g_2^{-1})_{\beta \bar{m}_B}. \end{aligned} \quad (2.32)$$

the crossed correlator is computed as

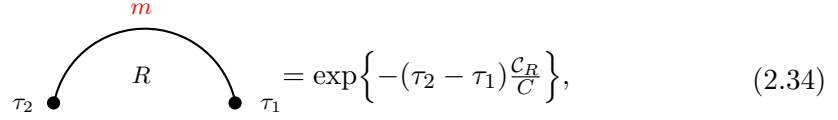
$$\text{Tr} \left[e^{-\beta H} R_B(\hat{g}_4)_{m_B \beta} R_A(\hat{g}_3)_{m_A \alpha} R_B(\hat{g}_2^{-1})_{\beta \bar{m}_B} R_A(\hat{g}_1^{-1})_{\alpha \bar{m}_A} \right]. \quad (2.33)$$

Also this computation is deferred to the Appendix D. The results of these computations match the previous expressions.

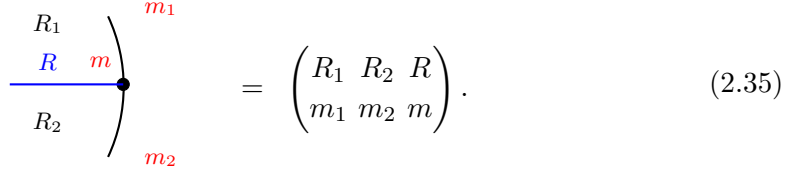
2.3 Diagrammatic Expansion

The calculations of section 2.1 can be summarized in a set of diagrammatic rules which can be used to write down any amplitude of an arbitrary number of boundary-anchored Wilson line insertions in BF.

- The starting point is just the disk on which the Wilson lines are drawn.
- Each region in the disk is assigned an irrep R_i , and contributes a weight $\dim R_i$. Assign a m_i label to each boundary segment. Eventually these labels R_i and m_i are to be summed over.
- Each boundary segment carries a Hamiltonian propagation factor (2.7) proportional to the length L_i of the relevant segment i . Each intersection of an endpoint of a Wilson line with the boundary has associated with it 3 irreps and 3 labels and is weighted with the $3j$ -symbol associated with these labels.

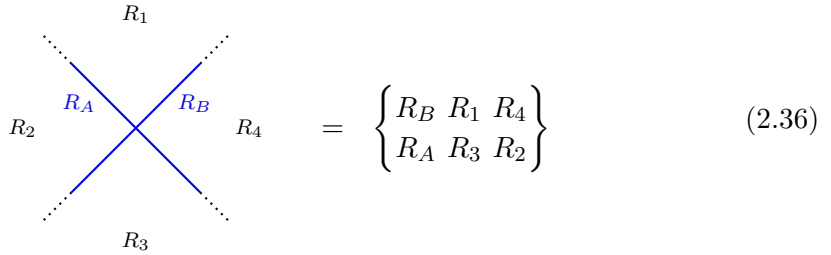


$$\begin{array}{c} m \\ \text{---} \text{---} \text{---} \\ \text{---} \text{---} \text{---} \\ \tau_2 \bullet \quad \quad \quad \bullet \tau_1 \\ R \end{array} = \exp\left\{- (\tau_2 - \tau_1) \frac{C_R}{C}\right\}, \quad (2.34)$$



$$\begin{array}{c} R_1 \\ \text{---} \text{---} \text{---} \\ R \\ \text{---} \text{---} \text{---} \\ R_2 \end{array} \begin{array}{c} m_1 \\ \text{---} \\ m \\ \text{---} \\ m_2 \end{array} = \begin{pmatrix} R_1 & R_2 & R \\ m_1 & m_2 & m \end{pmatrix}. \quad (2.35)$$

- Each crossing of two Wilson lines is associated with 6 irreps and is weighed with the appropriate $6j$ -symbol (2.25)

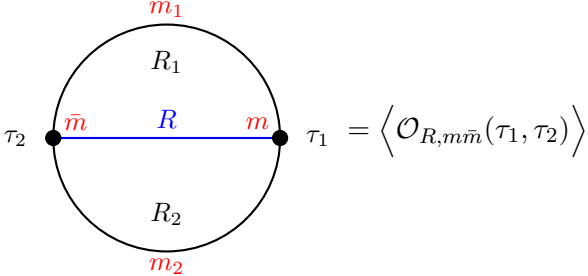


$$\begin{array}{c} R_1 \\ \text{---} \text{---} \text{---} \\ R_A \\ \text{---} \text{---} \text{---} \\ R_2 \end{array} \begin{array}{c} R_B \\ \text{---} \text{---} \text{---} \\ R_4 \\ \text{---} \text{---} \text{---} \\ R_3 \end{array} = \begin{pmatrix} R_B & R_1 & R_4 \\ R_A & R_3 & R_2 \end{pmatrix} \quad (2.36)$$

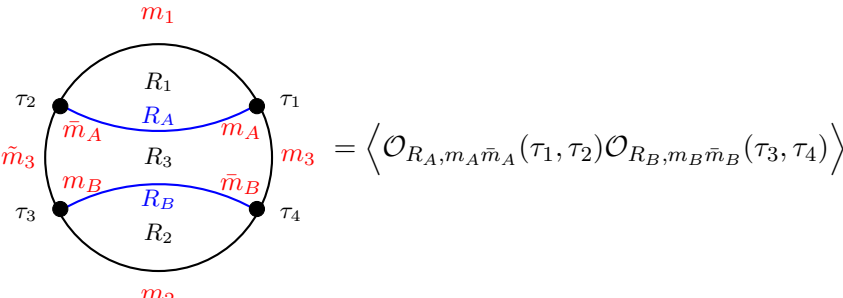
These rules agree with the diagrammatic rules established for the correlators of bilocals in particle-on-a-group (2.29) in [24], which confirms the full equivalence of BF correlators and particle-on-a-group correlators through the dictionary (2.29).

Some examples are instructive to clarify the above rules. Using (2.29), the two-point

function and four-point function are diagrammatically:

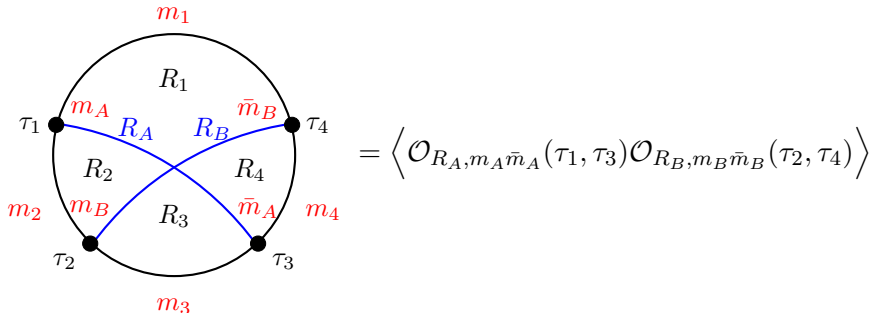


$$= \sum_{R_1, R_2} \dim R_1 \dim R_2 e^{-\tau_{21} \frac{c_{R_1}}{c}} e^{-(\beta - \tau_{21}) \frac{c_{R_2}}{c}} \times \sum_{m_1, m_2} \begin{pmatrix} R_1 & R & R_2 \\ m_1 & m & m_2 \end{pmatrix} \begin{pmatrix} R_1 & R & R_2 \\ m_1 & \bar{m} & m_2 \end{pmatrix}, \quad (2.37)$$



$$= \sum_{R_1, R_2, R_3, R_4} \prod_i \dim R_i e^{-a\tau_{21} c_{R_1}} e^{-a\tau_{32} c_{R_3}} e^{-a\tau_{43} c_{R_2}} e^{-a(\beta - \tau_{14}) c_{R_3}} \times \sum_{m_1, m_2, m_3, \tilde{m}_3} \begin{pmatrix} R_1 & R_A & R_3 \\ m_1 & m_A & m_3 \end{pmatrix} \begin{pmatrix} R_1 & R_A & R_3 \\ m_1 & \tilde{m}_A & \tilde{m}_3 \end{pmatrix} \begin{pmatrix} R_2 & R_B & R_3 \\ m_2 & m_B & \tilde{m}_3 \end{pmatrix} \begin{pmatrix} R_2 & R_B & R_3 \\ m_2 & \tilde{m}_B & m_3 \end{pmatrix}. \quad (2.38)$$

A further example is the expectation value of two crossing Wilson lines, or equivalently the product of two bilocal operators $\mathcal{O}_{R_A, m_A \bar{m}_A}(\tau_1, \tau_3)$ and $\mathcal{O}_{R_B, m_B \bar{m}_B}(\tau_2, \tau_4)$, with time-ordering $\tau_1 < \tau_2 < \tau_3 < \tau_4$:



$$= \sum_{R_1, R_2, R_3, R_4} \prod_i \dim R_i e^{-a\tau_{21} c_{R_2}} e^{-a\tau_{32} c_{R_3}} e^{-a\tau_{43} c_{R_4}} e^{-a(\beta - \tau_{14}) c_{R_1}} \times \left\{ \begin{matrix} R_B & R_1 & R_4 \\ R_A & R_3 & R_2 \end{matrix} \right\} \times \sum_{m_1, m_2, m_3, m_4} \begin{pmatrix} R_1 & R_A & R_2 \\ m_1 & m_A & m_2 \end{pmatrix} \begin{pmatrix} R_1 & R_B & R_4 \\ m_1 & \bar{m}_B & m_4 \end{pmatrix} \begin{pmatrix} R_2 & R_B & R_3 \\ m_2 & m_B & m_3 \end{pmatrix} \begin{pmatrix} R_3 & R_A & R_4 \\ m_3 & \bar{m}_A & m_4 \end{pmatrix} \quad (2.39)$$

Schematically writing this out in terms of local operators, using (2.29), we would be computing something like

$$\langle \overbrace{\mathcal{O}_1 \mathcal{O}_2 \mathcal{O}_3 \mathcal{O}_4} \rangle. \quad (2.40)$$

Such a configuration is closely related, but not equal to an out-of-time ordered (OTO) correlator, which in terms of local operators would be

$$\langle \overbrace{\mathcal{O}_1 \mathcal{O}_3 \mathcal{O}_2 \mathcal{O}_4} \rangle. \quad (2.41)$$

Technically, the only difference is in the exponential damping factors. For OTO correlators, the thermal circle in the diagram is to be interpreted as the *unfolded* time contour. Pragmatically, when going to OTO correlators, care must be taken in the exponential factors to ensure all of them are damped in Euclidean signature, in the end leading to a specific Lorentzian OTO correlator after Wick rotation [23, 25]. The diagram is

$$= \left\langle \mathcal{O}_{R_A, m_A \bar{m}_A}(\tau_1, \tau_2) \mathcal{O}_{R_B, m_B \bar{m}_B}(\tau_3, \tau_4) \right\rangle_{\text{OTO}}$$

$$= \sum_{R_1, R_2, R_3, R_4} \prod_i \dim R_i e^{-a\tau_{31}C_{R_2}} e^{-a\tau_{32}C_{R_3}} e^{-a\tau_{42}C_{R_4}} e^{-a(\beta-\tau_{41})C_{R_1}} \times \begin{Bmatrix} R_B & R_1 & R_4 \\ R_A & R_3 & R_2 \end{Bmatrix}$$

$$\times \sum_{m_1, m_2, m_3, m_4} \begin{pmatrix} R_1 & R_A & R_2 \\ m_1 & m_A & m_2 \end{pmatrix} \begin{pmatrix} R_1 & R_B & R_4 \\ m_1 & \bar{m}_B & m_4 \end{pmatrix} \begin{pmatrix} R_2 & R_B & R_3 \\ m_2 & m_B & m_3 \end{pmatrix} \begin{pmatrix} R_3 & R_A & R_4 \\ m_3 & \bar{m}_A & m_4 \end{pmatrix}, \quad (2.42)$$

with notably $\tau_{32} = L_3$ and not τ_{23} in the second exponential ensuring proper damping.

All of this demonstrates that the particle-on-a-group diagrams are to be interpreted as bulk BF Wilson line diagrams, a perspective that is not clear a priori when deriving these expressions with 2d CFT techniques [24].

3 Interlude: Non-Compact Groups

The above description is readily generalizable to non-compact groups, where one just uses the $3j$ - and $6j$ -symbols of the representations of the group. A new feature is the appearance of continuous representations, which require the replacement $\sum_R \dim R \rightarrow \int dR \rho(R)$, where the Plancherel measure $\rho(R)$ in the irrep R is to be used. The difficulty, as always, is to find out which representations actually appear in the Hilbert space.

Irreducible representations of a non-compact group are not all unitary. For our purposes,

only the unitary representations appear in the Peter-Weyl decomposition and hence in the Hilbert spaces of the models. It is particularly interesting at this point to turn the eye towards $\mathrm{SL}(2, \mathbb{R})$, which is closely linked to the gravitational systems. The unitary irreducible representations of $\mathrm{SL}(2, \mathbb{R})$ have all been classified. Depending on which $\mathfrak{sl}(2, \mathbb{R})$ generator one diagonalizes, one distinguishes the elliptic basis (\mathcal{J}^3), the hyperbolic basis (\mathcal{J}^2) and the parabolic basis ($\mathcal{J}^+ \equiv \mathcal{J}^1 + i\mathcal{J}^2$). Ordinarily, the elliptic basis is preferred, as the eigenvalue indices m and n are discrete in that case.

- Principal Continuous Representation \mathcal{C}_s , with $j = -1/2 + is$, $m \in \mathbb{Z}$.
- Complementary Representation \mathcal{E}_j , with $-1 < j < 0$, $m \in \mathbb{Z}$.
- Principal Discrete Representation (highest or lowest weight) \mathcal{D}_ℓ^\pm , with $\ell \in \frac{\mathbb{N}}{2}$, $m = \pm\ell, \pm(\ell + 1), \dots$
- Trivial Representation $j = 0$.

Any $\psi \in L^2(G)$ can be decomposed by the Plancherel formula as

$$\psi(g) = \int_0^{+\infty} ds s \tanh(\pi s) \sum_{m,n \in \mathbb{Z}} c_{mn}^s R_{-\frac{1}{2}+is, mn}(g) + \sum_{\ell=0}^{+\infty} \sum_{m,n=\pm\ell}^{\pm\infty} \left(\ell + \frac{1}{2}\right) c_{mn}^\ell R_{\ell, mn}^\pm(g), \quad (3.1)$$

where the first term contains the principal continuous representations \mathcal{C}_s , and the second term contains both the lowest and highest weight discrete representation \mathcal{D}_ℓ^\pm . The complementary continuous representation and trivial representation, despite being unitary, are not in $L^2(G)$.

To obtain gravity, the crux of the matter will be to impose suitable constraints on this system (the parabolic basis will be most convenient for this), and find out which representations survive.

4 Schwarzian Theory

In this section we discuss the gravitational analogue of the story of section 2. We start by recapitulating some of the relevant expressions from 3d / 2d holography before specializing to 2d / 1d holography. Figure 1 summarizes the relation between the theories relevant for this section. The discussion of this section relies heavily on how precisely the gravitational sector is encoded within gauge theory in these models. By identifying the Schwarzian as a constrained particle on $\mathrm{SL}(2, \mathbb{R})$ [15, 36], we are able to generalize the conclusions of section 2 and identify boundary-anchored Wilson lines in JT gravity - which is just constrained $\mathrm{SL}(2, \mathbb{R})$ BF theory [15] - as bilocal operators in the Schwarzian. The $6j$ -symbols, associated to crossing Wilson lines in the bulk, appear in Schwarzian OTO correlators and account for gravitational shockwaves.¹⁰ Since $\mathrm{SL}(2, \mathbb{R})$ BF and by extension $\mathrm{SL}(2, \mathbb{R})$ YM

¹⁰In particular, in [25] it was proven that precisely these $\mathrm{SL}(2, \mathbb{R})$ $6j$ -symbols contain the entire eikonal gravitational shockwave expression in the semiclassical $C \rightarrow \infty$ regime.

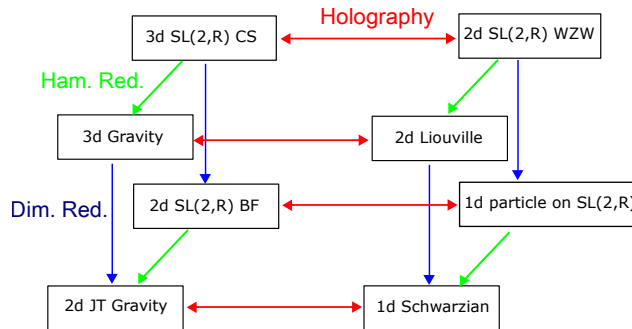


Figure 8. Relation through holography, the Schwarzian limit (dimensional reduction), and Hamiltonian reduction of eight theories.

is less understood than their rational cousins, this section serves a double goal: we provide a Wilson line perspective on Schwarzian correlators by assuming the calculations of boundary-anchored Wilson lines in constrained $\text{SL}(2, \mathbb{R})$ BF theory are structurally equivalent to those of their rational cousins, and *prove* the resulting diagrammatic rules by explicitly matching with Schwarzian correlators.

4.1 Liouville as Constrained WZW

It is well-known that 3d gravity with negative cosmological constant can be written as two copies of $\text{SL}(2, \mathbb{R})$ CS, or equivalently as a non-chiral $\text{SL}(2, \mathbb{R})$ WZW model. Imposing the metric to be asymptotically AdS_3 constrains the $\text{SL}(2, \mathbb{R})$ CS gauge fields. The result is that the boundary $\text{SL}(2, \mathbb{R})$ WZW model is also constrained / gauged, reducing the symmetry from $\text{SL}(2, \mathbb{R})$ Kac-Moody to Virasoro and the action to the Liouville action.

Consider a 2d worldsheet (z, \bar{z}) on which one defines five fields $(\phi, \gamma_L, \gamma_R, \beta, \bar{\beta})$ with Lagrangian:

$$\mathcal{L} = \partial\phi\bar{\partial}\phi + \beta\bar{\partial}\gamma_L + \bar{\beta}\partial\gamma_R + \beta\bar{\beta}e^{2\phi}. \quad (4.1)$$

This is the Wakimoto representation of the $\text{SL}(2, \mathbb{R})$ WZW model [53]. Integrating out β and $\bar{\beta}$ through their equations of motion $\bar{\partial}\gamma_L + \bar{\beta}e^{2\phi} = 0$, $\partial\gamma_R + \beta e^{2\phi} = 0$, one retrieves the standard WZW $\text{SL}(2, \mathbb{R})$ Lagrangian for a metric $ds^2 = d\phi^2 + e^{-2\phi}d\gamma_L d\gamma_R$ [54–56]:

$$\mathcal{L} = \partial\phi\bar{\partial}\phi + \bar{\partial}\gamma_L\partial\gamma_R e^{-2\phi}, \quad (4.2)$$

Liouville is obtained from $\text{SL}(2, \mathbb{R})$ WZW by means of a Drinfeld-Sokolov Hamiltonian reduction [39, 57–59]. Specifically, to obtain Liouville from $\text{SL}(2, \mathbb{R})$ WZW one constrains one component of the holomorphic Kac-Moody currents \mathcal{J}^a and one component of the antiholomorphic currents $\bar{\mathcal{J}}^a$ as [57]:

$$\mathcal{J}^- = \sqrt{\mu}, \quad \bar{\mathcal{J}}^+ = \sqrt{\mu}, \quad (4.3)$$

for some constant μ that will turn out to be the Liouville cosmological constant. The constraints (4.3) emerge in the bulk as the constraints that force the metric to be asymptotically AdS_3 [60]. Imposing these constraints in a proper path integral manner is done

by gauging the parabolic subgroup of $\mathrm{SL}(2, \mathbb{R})$ in the gauged WZW model.¹¹

At the level of the action, the equivalence is readily observed using the Wakimoto formulation of $\mathrm{SL}(2, \mathbb{R})$ WZW (4.1). The system (4.1) has conserved Kac-Moody currents:

$$\begin{aligned}\mathcal{J}^- &= \beta, & \bar{\mathcal{J}}^- &= \bar{\beta}\gamma_R^2 - 2\gamma_R\bar{\partial}\phi - \bar{\partial}\gamma_R, \\ \mathcal{J}^0 &= \beta\gamma_L - \partial\phi, & \bar{\mathcal{J}}^0 &= \bar{\beta}\gamma_R - \bar{\partial}\phi, \\ \mathcal{J}^+ &= \beta\gamma_L^2 - 2\gamma_L\partial\phi - \partial\gamma_L, & \bar{\mathcal{J}}^+ &= \bar{\beta}.\end{aligned}\tag{4.4}$$

Imposing (4.3) at the level of the action and substituting this in (4.1), one obtains the Liouville Lagrangian:

$$\mathcal{L} = \partial\phi\bar{\partial}\phi + \mu e^{2\phi}.\tag{4.5}$$

Correlation functions can also be linked to each other, though this requires a bit more effort [63]. The procedure identifies the parameters of Liouville and WZW as:

$$b^2 = \frac{1}{k-2}.\tag{4.6}$$

In what follows we will be interested solely in a particular dimensional reduction of this story, in which we also take $b \rightarrow 0$ or equivalently $k \rightarrow \infty$.¹²

4.2 Schwarzian as Constrained Particle-on-a-group

The dimensional reduction of Liouville while taking simultaneously $b \rightarrow 0$ results in the Schwarzian theory [23, 24], dual to JT gravity. Similarly, the dimensional reduction while taking simultaneously $k \rightarrow \infty$ of $\mathrm{SL}(2, \mathbb{R})$ WZW results in a particle on $\mathrm{SL}(2, \mathbb{R})$, dual to $\mathrm{SL}(2, \mathbb{R})$ BF. We are interested here in the embedding of the Schwarzian in $\mathrm{SL}(2, \mathbb{R})$ BF. At the level of the action, this was already examined in [23], where it was demonstrated that the Schwarzian

$$L = \{f, \tau\},\tag{4.7}$$

can be rewritten through integrating in and out Lagrange multipliers both as the action of a particle on the $\mathrm{SL}(2, \mathbb{R})$ group manifold:¹³

$$L = \frac{1}{2}\dot{\phi}^2 + \gamma_L\dot{\gamma}_R e^{-\phi},\tag{4.8}$$

and as the 1d Liouville model:

$$L = \frac{1}{2}\dot{\phi}^2 - \mu e^{\phi}.\tag{4.9}$$

¹¹Alternatively, one can also start with a chiral $\mathrm{SL}(2, \mathbb{R})$ WZW; this is explained in detail in [61, 62] where the procedure results first in the Virasoro coadjoint orbit action, which in turn is directly related to the Liouville path integral between branes, producing a single Virasoro character.

¹²As a check on (4.6), note that at large k the central charge $c = 6k$ of the constrained $\mathrm{SL}(2, \mathbb{R})$ WZW model matches the Liouville central charge, and that the conformal weight $h = P^2 + \frac{1}{4b^2}$ of the Liouville states at small b matches the weights $h = \frac{j(j+1)}{k-2} + \frac{k}{4}$ of the $\mathrm{SL}(2, \mathbb{R})$ principal continuous irrep primaries $j = -\frac{1}{2} + is$, upon identification of the Liouville momentum as $P = bs$.

¹³Here the phase space is larger compared to the Schwarzian or 1d Liouville.

Here we go deeper, and demonstrate that the perspective of the Schwarzian as constrained particle on $\mathrm{SL}(2, \mathbb{R})$ is powerful enough to allow a full solution of the quantum model.

The first goal is to identify the embedding of the Schwarzian states in the $\mathrm{SL}(2, \mathbb{R})$ BF spectrum. Let us first return thereto to the Liouville / $\mathrm{SL}(2, \mathbb{R})$ WZW story. The Hilbert space of $\mathrm{SL}(2, \mathbb{R})$ WZW consists of states $|j, m\bar{m}, n\bar{n}\rangle$, with j labeling either a principal continuous or a discrete irrep of $\mathrm{SL}(2, \mathbb{R})$. The labels m and \bar{m} specify a certain state in the zero-grade Hilbert space of $\mathrm{SL}(2, \mathbb{R})$, generated by \mathcal{J}_0^a . Applying the raising operators \mathcal{J}_{-n}^a constructs the entire module, associated with a specific irrep j .

After Hamiltonian reduction, only the principal continuous spectrum survives as normalizable solutions to the constrained $\mathrm{SL}(2, \mathbb{R})$ Casimir differential equation.¹⁴ Consider now the module $|k, m\bar{m}, n\bar{n}\rangle$ for fixed k referring to a principal continuous series irrep of $\mathrm{SL}(2, \mathbb{R})$ $j = -\frac{1}{2} + ik$. As shown in [39], the effect of the Drinfeld-Sokolov Hamiltonian reduction is to map such a module to a single Virasoro Verma module associated with the same state k : these are states $|k, n\bar{n}\rangle$ where now k is a Virasoro primary and n and \bar{n} label Virasoro descendants.

Further taking the double-scaling limit to descend to the 1d theory, requires $n = \bar{n} = 0$ as descendants are suppressed. Explicitly, to obtain the spectrum of Schwarzian states, we impose the Hamiltonian reduction constraints (4.3) on the $\mathrm{SL}(2, \mathbb{R})$ quantum mechanics states $|j, m\bar{m}\rangle$. As explained in Appendix E and [57] this forces us to consider states in the mixed parabolic basis where the labels m, \bar{m} are continuous eigenvalues of $\mathcal{J}^-, \bar{\mathcal{J}}^+$ respectively which will henceforth be labeled by Greek letters $\nu, \lambda \dots$. If we set $\mathcal{J}^- = \nu$ and $\bar{\mathcal{J}}^+ = \lambda$, the constraints show that the Schwarzian states $|k\rangle$ are diagonal $\mathrm{SL}(2, \mathbb{R})$ states with $\nu = \lambda = \sqrt{\mu}$:

$$|k\rangle = |k, \sqrt{\mu}, \sqrt{\mu}\rangle. \quad (4.10)$$

4.3 Correlation Functions in Constrained BF

We proceed by again calculating generic correlators of boundary-anchored Wilson lines in JT gravity or constrained $\mathrm{SL}(2, \mathbb{R})$ BF. Later on in section 4.4 we identify boundary-anchored Wilson lines through holography as bilocal operators in the Schwarzian theory. The match of all amplitudes discussed here with the Schwarzian amplitudes completes the proof of the dictionary.

4.3.1 Open Channel Description

We present again an open-channel basis description. Representation matrices are matrix elements $R_{k, \nu\lambda}(g) = \langle k, \nu | g | k, \lambda \rangle$ and can be found in the available literature [64]. In Appendix E we elaborate on the mixed parabolic basis required to describe Schwarzian quantum mechanics, and on the parameterization relevant for this work.¹⁵ This Appendix also provides with some of the technical calculations underlying the main story presented here.

¹⁴This is discussed in more detail in section 4.3.1 and Appendix E.3.

¹⁵There appears to be about as many ways to choose and parameterize the basis and the group element of $\mathrm{SL}(2, \mathbb{R})$ as there are “ways to die in the west”.

From (4.10) we find the relevant representation matrix elements for constrained $\text{SL}(2, \mathbb{R})$ as $R_{k, \sqrt{\mu}, \sqrt{\mu}}(g)$. If we coordinatize the $\text{SL}(2, \mathbb{R})$ group manifold as

$$ds^2 = d\phi^2 + e^{-2\phi} d\gamma_L d\gamma_R, \quad (4.11)$$

the representation matrices of the continuous series $\text{SL}(2, \mathbb{R})$ irreps in the mixed parabolic basis are explicitly [57, 64]:

$$R_{k, \nu\lambda}(g) \equiv \langle \nu_L | g(\phi, \gamma_L, \gamma_R) | \lambda_R \rangle = 2 \left(-\frac{\lambda}{\nu} \right)^{ik} e^\phi K_{2ik}(\sqrt{\nu\lambda} e^\phi) e^{i\nu\gamma_L + i\lambda\gamma_R}. \quad (4.12)$$

The normalization of the representation matrices is fixed by the normalization of the bra and the ket discussed in Appendix E. Specifying to the Liouville case of interest we obtain:

$$R_{k, \sqrt{\mu}, \sqrt{\mu}}(g) = e^\phi K_{2ik}(\sqrt{\mu} e^\phi) e^{i\sqrt{\mu}(\gamma_L + \gamma_R)}. \quad (4.13)$$

The metric (4.11) comes with integration measure $d\phi d\gamma_L d\gamma_R e^{-2\phi}$. Due to the relation

$$\int_{-\infty}^{+\infty} d\phi K_{2ik}(\sqrt{\mu} e^\phi) K_{2ik'}(\sqrt{\mu} e^\phi) = \frac{\pi^2}{8k \sinh(2\pi k)} \delta(k - k'), \quad (4.14)$$

these matrix elements satisfy the orthogonality relations:

$$\int dg R_{k, \nu\lambda}(g) R_{k', \nu'\lambda'}(g^{-1}) = \frac{\pi^2}{8k \sinh(2\pi k)} \delta(k - k') \delta(\nu - \nu') \delta(\lambda - \lambda'). \quad (4.15)$$

This relation is the analogue of (2.5) and we identify the analogue of $\dim k$ for this non-compact example as:

$$\boxed{\dim k = k \sinh 2\pi k}. \quad (4.16)$$

The open channel principal continuous series $\text{SL}(2, \mathbb{R})$ wavefunctions in the mixed parabolic basis are the analogue of (2.5):

$$\langle g | k, \nu\lambda \rangle = \sqrt{k \sinh 2\pi k} R_{k, \nu\lambda}(g), \quad (4.17)$$

and are orthogonal with respect to the measure $dg = d\phi d\gamma_L d\gamma_R e^{-2\phi}$. Note that the density of states (4.16) differs from the standard $\text{SL}(2, \mathbb{R})$ Plancherel measure, and fully arises from the Hamiltonian reduction step which forces us to construct matrix elements between states in two different bases as explained in Appendix E. The observation that this is indeed the analogue of $\dim k$ solidifies by looking back to 2d Liouville, where this role is played by the S_{0k} elements of the modular S-matrix. For irreps k of compact Lie groups, S_{0k} reduces to the dimension $\dim k$ of the irrep in the minisuperspace limit, which matches with the $k \sinh 2\pi k$ measure in the non-compact case at hand [23].

In all of our computations, the only effect of the γ_L - and γ_R -integrals is to create a delta-function on the ν 's and λ 's. Stripping off the γ -dependence, the normalized wavefunctions can be identified with the Liouville wavefunctions [65–67]:

$$\langle \phi | k \rangle = \sqrt{k \sinh 2\pi k} K_{2ik}(\sqrt{\mu} e^\phi), \quad (4.18)$$

now with the flat integration measure $d\phi$. In fact, imposing the constraints directly on the $\text{SL}(2, \mathbb{R})$ Casimir differential equation, one lands on the 1d Liouville eigenvalue problem, i.e. the Schrödinger equation for a particle in an exponential potential $V(\phi) = \mu e^{2\phi}$. The latter of course has only a continuous spectrum of normalizable modes, explaining immediately why only continuous representations survive the Hamiltonian reduction. We give some more formulas accompanying this discussion in Appendix E.3.

Knowledge of the wavefunctions and matrix elements is sufficient to calculate the disk amplitude of JT gravity. Consider the disk amplitude from Figure 4, where now the boundary states are characterized by some $\text{SL}(2, \mathbb{R})$ group elements g and h :

$$Z_{\text{disk}}(g, h) = \langle g | e^{-TH} | h \rangle. \quad (4.19)$$

The Hamiltonian is boundary-localized and is the Casimir in the principal continuous representation of $\text{SL}(2, \mathbb{R})$:

$$H(k) = \frac{\mathcal{C}_k}{C} = \frac{k^2}{C}, \quad (4.20)$$

where the constant shift $1/4$ of the Casimir was dropped.¹⁶ Inserting a complete set of states $|k\rangle$ of the constrained theory, we obtain:

$$Z_{\text{disk}}(g, h) = \int dk \langle g | k \rangle \langle k | h \rangle e^{-TH(k)} = \int d\mu(k) R_{k, \sqrt{\mu}\sqrt{\mu}}(g) R_{k, \sqrt{\mu}\sqrt{\mu}}(h) e^{-TH(k)}, \quad (4.21)$$

where we re-introduced the measure $d\mu(k) = k \sinh 2\pi k dk$. For compact groups we noted that the physical boundary of BF was characterized by $g = h = \mathbf{1}$. For JT gravity, we are using a mixed parabolic basis. We explain in Appendix E in equation (E.33) that the analogous statement, in the Gauss decomposition of the $\text{SL}(2, \mathbb{R})$ group element (E.27), is that $\phi \rightarrow \infty$, $\gamma_L = e^\phi = -\gamma_R$ to find the identity element. Indeed, in this region we use the asymptotics $K_{2ik}(z) \rightarrow \sqrt{\frac{\pi}{2z}} e^{-z}$, and find $R_{k, \sqrt{\mu}\sqrt{\mu}}(g) \rightarrow \sqrt{\frac{\pi}{2\sqrt{\mu}}} e^{\phi/2} e^{-e^\phi}$, independent of k , which can hence be normalized away.

As for the compact case in section 2.1.1, there is an analogous description of the disk amplitude in the point defect channel of Figure 5. The boundary defect is now characterized by $\phi \rightarrow +\infty$, which is precisely the ZZ-brane boundary conditions, upon again identifying ϕ as the 1d Liouville field.

From (4.21), the amplitude of the empty disk is:

$$Z_{\text{disk}} = \int d\mu(k) e^{-\frac{\beta k^2}{C}}, \quad (4.22)$$

indeed matching the known Schwarzian partition function [24, 29].

¹⁶It drops out of expectation values when normalized by the partition function Z_{disk} .

4.3.2 Wilson Lines

As for compact groups, a Wilson line segment in an irrep j of $\text{SL}(2, \mathbb{R})$ with starting point and endpoint labeled by m respectively n is $R_{j, mn}$. Here we will be concerned with Wilson lines in a discrete series irrep $j = \ell$ of $\text{SL}(2, \mathbb{R})$ since, as we will discuss below, these are the only sensible ones and because they contain the Liouville operators $e^{2\ell\phi}$.

Let us start this discussion with a derivation of the $\text{SL}(2, \mathbb{R})$ $3j$ -symbols when one of the irreps is in the principal discrete series and the two others are in the principal continuous series. These are obtained using the analogue of equation (2.19):

$$\int dg R_{k_1, \nu_1 \nu_1}(g) R_{\ell, mm}(g) R_{k_2, \nu_2 \nu_2}(g) = \begin{pmatrix} k_1 & \ell & k_2 \\ \nu_1 & m & \nu_2 \end{pmatrix}^2, \quad (4.23)$$

where $dg = d\phi d\gamma_L d\gamma_R e^{-2\phi}$. The discrete series representation matrices of $\text{SL}(2, \mathbb{R})$ in the mixed parabolic basis are given by modified Bessel functions of the first kind [64]:

$$R_{\ell, mn}(g) = \langle m_L | g(\phi, \gamma_L, \gamma_R) | n_R \rangle = 2 \left(-\frac{m}{n} \right)^{\ell + \frac{1}{2}} e^\phi I_{2\ell-1}(\sqrt{mn}e^\phi) e^{im\gamma_L + im\gamma_R}. \quad (4.24)$$

These are eigenfunctions of the same differential equation as the Macdonald functions (4.12) and thus also eigenfunctions of the $\text{SL}(2, \mathbb{R})$ Casimir. Note that the integral (4.23) is ill-defined for $j \neq \ell$, such that only operators with $j = \ell$ are to be considered in this gravitational setting. This separation of states (continuous representations) and operators (discrete representations) happens naturally for the Schwarzian as for its Liouville ancestor [68] by the specific boundary conditions singled out in the Hamiltonian reduction of $\text{SL}(2, \mathbb{R})$.

Inserting this and (4.12) in (4.23) reduces the computation to the integral

$$\mathcal{I} = \int_0^{+\infty} dx K_{2ik_1}(\nu_1 x) I_{2\ell-1}(mx) K_{2ik_2}(\nu_2 x). \quad (4.25)$$

This integral was calculated by [69, 70] with the result:¹⁷

$$\mathcal{I} = \frac{m^{2\ell} \nu_1^{2ik_1}}{\nu_2^{2ik_1+2\ell}} \frac{\Gamma(\ell \pm ik_1 \pm ik_2)}{\Gamma(2\ell)^2} {}_2F_1 \left(\ell + ik_1 + ik_2, \ell + ik_1 - ik_2, 2\ell; -\frac{m}{\nu_1} \right)^2. \quad (4.27)$$

Combining this with the γ_L and γ_R integrals, the $3j$ -symbols of $\text{SL}(2, \mathbb{R})$ in the parabolic basis are thus

$$\begin{aligned} \begin{pmatrix} k_1 & \ell & k_2 \\ \nu_1 & m & \nu_2 \end{pmatrix} &= \frac{m^\ell}{\sqrt{\Gamma(2\ell)}} \frac{\nu_1^{ik_1}}{\nu_2^{ik_1}} \left(\frac{\Gamma(\ell \pm ik_1 \pm ik_2)}{\Gamma(2\ell)} \right)^{\frac{1}{2}} \\ &\quad \times {}_2F_1 \left(\ell + ik_1 + ik_2, \ell + ik_1 - ik_2, 2\ell; -\frac{m}{\nu_1} \right) \delta(\nu_1 - m - \nu_2). \end{aligned} \quad (4.28)$$

¹⁷We use the \pm notation to indicate taking the product of all combinations of signs. In this case:

$$\Gamma(\ell \pm ik_1 \pm ik_2) \equiv \Gamma(\ell + ik_1 + ik_2) \Gamma(\ell + ik_1 - ik_2) \Gamma(\ell - ik_1 + ik_2) \Gamma(\ell - ik_1 - ik_2). \quad (4.26)$$

The same $3j$ -symbols for $\text{SL}(2, \mathbb{R})$ in the parabolic basis were obtained in the mathematics literature in [71].

Let us now consider an insertion of a boundary-anchored Wilson line. Using the open-channel propagation through the bulk regions we are led to consider the integral

$$\int dg R_{k_1, \sqrt{\mu}\sqrt{\mu}}(g) R_{\ell, mn}(g) R_{k_2, \sqrt{\mu}\sqrt{\mu}}(g). \quad (4.29)$$

This is proportional to $\delta(m)\delta(n)$. Notice that in the limit $m = n = \epsilon \rightarrow 0$, the discrete series matrix elements (4.24) depend only on ϕ and behave as:

$$R_{\ell, \epsilon\epsilon}(g) = R_{\ell, \epsilon\epsilon}(\phi) = \frac{\epsilon^{2\ell}}{\Gamma(2\ell)} e^{2\ell\phi}, \quad (4.30)$$

where one recognizes the operator spectrum $e^{2\ell\phi}$ of Liouville. This is further evidence that in this gravitational setup, one should only analyze Wilson lines in the discrete series irreps of $\text{SL}(2, \mathbb{R})$.

The $3j$ -symbols that appear in the JT calculation when a Wilson line touches the boundary are thus obtained from

$$\int dg R_{k_1, \sqrt{\mu}\sqrt{\mu}}(g) R_{\ell, 00}(g) R_{k_2, \sqrt{\mu}\sqrt{\mu}}(g) = \begin{pmatrix} k_1 & \ell & k_2 \\ \sqrt{\mu} & 0 & \sqrt{\mu} \end{pmatrix}^2. \quad (4.31)$$

The integral over ϕ can be evaluated using formula (6.576) of [72]:

$$\int_{-\infty}^{+\infty} d\phi e^{2\ell\phi} K_{2ik_1}(\sqrt{\mu}e^\phi) K_{2ik_2}(\sqrt{\mu}e^\phi) = \frac{\Gamma(\ell \pm ik_1 \pm ik_2)}{\Gamma(2\ell)}. \quad (4.32)$$

The γ_L and γ_R plane wave integrals only give a momentum conserving $\delta(0)^2$, a factor which we remove by hand in the Hamiltonian reduction, but which is indeed present in the $\text{SL}(2, \mathbb{R})$ Clebsch-Gordan coefficients. Therefore the $3j$ -symbols relevant for JT gravity and the Schwarzian are:

$$\boxed{\begin{pmatrix} k_1 & \ell & k_2 \\ \sqrt{\mu} & 0 & \sqrt{\mu} \end{pmatrix}} = \left(\frac{\Gamma(\ell \pm ik_1 \pm ik_2)}{\Gamma(2\ell)} \right)^{\frac{1}{2}}, \quad (4.33)$$

which can immediately be identified with the Schwarzian diagrammatic rule [23] and is to be compared with (2.35). It is instructive to compare at this point to the minisuperspace computation of the Liouville CFT three-point function. This results in the same integral (4.32) to be performed. Indeed, the bulk minisuperspace regime of Liouville yields the wavefunctions

$$\langle \phi | k \rangle = \frac{K_{2ik}(\sqrt{\mu}e^\phi)}{\Gamma(2ik)}.$$

Acknowledging that

$$\frac{1}{|\Gamma(2ik)|^2} = k \sinh 2\pi k = \dim k, \quad (4.34)$$

we see that these only differ by (4.18) by a phase factor, which is irrelevant. Matrix elements of constrained $\text{SL}(2, \mathbb{R})$ can directly be identified with Liouville wavefunctions. We obtain the precise analogue of the relation (C.16):

$$\langle k_2, \sqrt{\mu}, \sqrt{\mu} | \mathcal{O}_{\ell,00} | k_1, \sqrt{\mu}, \sqrt{\mu} \rangle = \sqrt{\dim k_1} \sqrt{\dim k_2} \begin{pmatrix} k_1 & \ell & k_2 \\ \sqrt{\mu} & 0 & \sqrt{\mu} \end{pmatrix}^2. \quad (4.35)$$

We have now acquired the necessary tools to calculate from the ground up generic configurations of Wilson lines in JT gravity i.e. constrained $\text{SL}(2, \mathbb{R})$ BF theory. A single Wilson line in discrete series irrep ℓ from boundary to boundary is just $R_{\ell,00}(g)$. Following formula (4.31) and the expression for the disk amplitude with a generic boundary (4.21), each endpoint of a Wilson lines on the boundary will contribute the $\text{SL}(2, \mathbb{R})$ $3j$ -symbol (4.33).

What happens on a bulk intersection of two Wilson lines? We would need an analogue of equation (2.24) to decompose the Hilbert space into two segments. This requires a more thorough discussion of $\text{SL}(2, \mathbb{R})$ representation theory in the parabolic basis, and we defer the treatment to Appendix E.4. Barring some details, the computation is essentially the same as that of the compact case, and leads to the appearance of a $6j$ -symbol at the intersection of crossing Wilson lines. The $6j$ -symbols of $\text{SL}(2, \mathbb{R})$ are obtained in the usual manner as an integral over all labels m_i of products of four generic $\text{SL}(2, \mathbb{R})$ $3j$ -symbols (4.28). Note that the Schwarzian $3j$ -symbols appear as a m_i -independent multiplicative factor in (4.28). The result for the $6j$ -symbol of $\text{SL}(2, \mathbb{R})$ with 2 discrete and 4 continuous representation labels has appeared in the mathematical literature before [73]. It also agrees with formula (5.13) in [23], determined from the 2d Liouville braiding R -matrix:

$$\left\{ \begin{matrix} \ell_1 & k_2 & k_1 \\ \ell_2 & k_4 & k_3 \end{matrix} \right\} = (\Gamma(\ell_1 \pm ik_2 \pm ik_1) \Gamma(\ell_2 \pm ik_2 \pm ik_3) \Gamma(\ell_1 \pm ik_4 \pm ik_3) \Gamma(\ell_2 \pm ik_4 \pm ik_1))^{\frac{1}{2}} \\ \times \mathbb{W}(k_1, k_3; \ell_1 + ik_4, \ell_1 - ik_4, \ell_2 - ik_2, \ell_2 + ik_2), \quad (4.36)$$

where $\mathbb{W}(\alpha, \beta; a, b, c, d)$ is the Wilson function [73, 74].¹⁸

4.4 Holography in Constrained BF

We proceed as in the compact case of section 2.2 by deriving the boundary Schwarzian action and bilocal operator vertex, directly from the bulk constrained chiral $\text{SL}(2, \mathbb{R})$ BF action and Wilson lines. The relation between the bulk $\text{SL}(2, \mathbb{R})$ BF theory and the boundary Schwarzian was given essentially in [36], which we phrase here in our language. As before, we start with the BF-action (2.1), and integrating out the bulk χ forces the connection A to be flat.

¹⁸Explicitly this is:

$$\mathbb{W}(\alpha, \beta; a, b, c, d) \equiv \frac{\Gamma(d-a) {}_4F_3 \left[\begin{matrix} a+i\beta & a-i\beta & \tilde{a}+i\alpha & \tilde{a}-i\alpha \\ a+b & a+c & 1+a-d \end{matrix} ; 1 \right]}{\Gamma(a+b)\Gamma(a+c)\Gamma(d\pm i\beta)\Gamma(\tilde{d}\pm i\alpha)} + (a \leftrightarrow d). \quad (4.37)$$

The gravitational boundary conditions gravely influence the resulting boundary dynamics, restricting the degrees of freedom. Going up one dimension, in chiral $\text{SL}(2, \mathbb{R})$ Chern-Simons in coordinates (τ, ϕ, r) , the gravitational boundary conditions are more restrictive than in the compact case, and are $(z = \tau + \phi, \bar{z} = \tau - \phi)$:¹⁹

$$A_z|_{r \rightarrow \infty} = iJ^- + T(\tau)iJ^+ = \begin{pmatrix} 0 & T(\tau) \\ 1 & 0 \end{pmatrix}, \quad A_{\bar{z}}|_{r \rightarrow \infty} = 0, \quad (4.38)$$

or

$$A_\tau|_{r \rightarrow \infty} = A_\phi|_{r \rightarrow \infty} = \begin{pmatrix} 0 & T(\tau) \\ 1 & 0 \end{pmatrix}. \quad (4.39)$$

Upon dimensional reduction to BF theory, as $A_\phi = \chi$ this constrains $\chi|_{\text{bdy}}$. Integrating out the bulk χ , one writes down the resulting BF boundary action:

$$L = H = \frac{1}{2} \text{Tr} \chi A_\tau = T(\tau), \quad (4.40)$$

identifying the quantity $T(\tau)$ with both the total energy H in the spacetime, and the Lagrangian L . The remaining degrees of freedom in the theory are $T(\tau)$ and are path-integrated over. This is the analogue of $g(\tau)$ for the unconstrained group models.

To rewrite the gravitational Wilson line in terms of this variable $T(\tau)$, we follow the recent approach of [75], which was done in the 3d / 2d case. A Wilson line in a discrete representation can be conveniently written in the Borel-Weil representation of the algebra (E.9). A discrete lowest weight state in representation j , labeled 0, has wavefunction

$$\langle x | j, 0 \rangle = \frac{1}{x^{2j}}, \quad \langle j, 0 | x \rangle = \delta(x). \quad (4.41)$$

The lowest weight diagonal matrix element of the Wilson line operator in this representation j , can then be written as

$$\begin{aligned} \mathcal{O}_j(\tau_1, \tau_2) &= \mathcal{W}_{j,00}(\tau_1, \tau_2) = \int dx \delta(x) \mathcal{P} e^{\int_{\tau_1}^{\tau_2} d\tau [\partial_x - T(\tau)(-x^2 \partial_x - 2jx)]} \frac{1}{x^{2j}} \\ &= \mathcal{P} e^{\int_{\tau_1}^{\tau_2} d\tau [\partial_x - T(\tau)(-x^2 \partial_x - 2jx)]} \frac{1}{x^{2j}} \Big|_{x=0}. \end{aligned} \quad (4.42)$$

The remaining technical computation was done in [75], by interpreting this path-ordered exponential as a Hamiltonian evolution operator, and then rewriting the latter in a path integral fashion. A field redefinition allows to write out (4.42) in a more suggestive manner. Upon introducing a new function $f(t)$, determined as the solution of

$$\{f, \tau\} = T(\tau), \quad (4.43)$$

the result can be written as

$$\mathcal{O}_\ell(\tau_1, \tau_2) = \left(\frac{f'_1 f'_2}{(f_1 - f_2)^2} \right)^\ell. \quad (4.44)$$

¹⁹For matrix representations of the generators see appendix E.

The field redefinition from the boundary condition $T(\tau)$ to $f(\tau)$ using equation (4.43) identifies f as the time reparametrization from the Poincaré patch into a generic frame of reference, due to a time-dependent bulk total energy $T(\tau)$ in spacetime at time τ . This field redefinition is only determined up to a $\text{SL}(2, \mathbb{R})$ redundancy. Moreover, demanding no infinite energy configuration $T(\tau) < \infty$ implies f' cannot have sign switches, meaning either $f' > 0$ or $f' < 0$ everywhere. As $\{f, \tau\}$ does not change upon $f' \rightarrow -f'$, we choose to take $f' > 0$ everywhere. This identifies the integration space as $\text{diff } \mathbb{R}/\text{SL}(2, \mathbb{R})$. The Lagrangian (4.40) becomes a Schwarzian derivative of f (4.7), and the Wilson line (4.44) becomes the Schwarzian bilocal operator.²⁰ The nonzero temperature parametrization can be found by imposing the additional boundary condition $T(\tau+\beta) = T(\tau)$, allowing a further reparametrization $f \rightarrow F = \tan \frac{\pi f}{\beta}$, and resulting in the integration space $\text{diff } S^1/\text{SL}(2, \mathbb{R})$.

As a check on this computation, for constant $T(\tau) = E$, representing black hole geometries in the bulk, the time-ordering \mathcal{P} becomes irrelevant, and the matrix exponential (4.42) can be directly computed using (E.2), with the result:

$$\mathcal{O}_\ell(\tau_1, \tau_2) = \left(\frac{\frac{E}{2}}{\sin^2 \left(\tau_{12} \sqrt{\frac{2}{E}} \right)} \right)^\ell, \quad (4.45)$$

which is precisely the two-point function on a thermal background with temperature $\frac{1}{\beta} = \frac{1}{\pi} \sqrt{\frac{E}{2}}$, matching the Hawking temperature of a mass E black hole in JT [16–19].

Summarizing we have re-established that the holographic dual of the constrained $\text{SL}(2, \mathbb{R})$ BF is the Schwarzian, but have also proven that Wilson lines in JT gravity are dual to the bilocal operators in the Schwarzian:

$$\boxed{\mathcal{W}_{\ell,00}(\tau_1, \tau_2) = \mathcal{O}_\ell(\tau_1, \tau_2) = \left(\frac{f'_1 f'_2}{(f_1 - f_2)^2} \right)^\ell}. \quad (4.46)$$

4.5 Diagrammatic Expansion

The calculation of a generic correlators of Wilson lines in JT gravity discussed in section 4.3 can be summarized in a set of diagrammatic rules very similar to those of section 2.3.

- The starting point is just the disk on which the Wilson lines are drawn.
- Each region in the disk is assigned a state k_i associated with a principal continuous series irrep of $\text{SL}(2, \mathbb{R})$, and contributes a weight $\dim k_i = k_i \sinh 2\pi k_i$. These labels k_i are integrated over.
- Each boundary segment carries a Schwarzian Hamiltonian propagation factor $e^{-L_i \frac{c_{k_i}}{C}}$. Each intersection of a Wilson line with the boundary has associated with it 3 $\text{SL}(2, \mathbb{R})$

²⁰The correct path integration measure over f will not be determined here, but follows from other perspectives, such as the 2d Liouville approach.

5 Concluding Remarks

Boundary-anchored Wilson lines in 2d BF theory were shown to map to bilocal operators in the particle-on-a-group model. By making explicit the embedding of the Schwarzian in constrained $SL(2, \mathbb{R})$ particle-on-a-group or equivalently the embedding of JT gravity in $SL(2, \mathbb{R})$ BF, we were able to provide a bulk derivation of correlators in the Schwarzian, relying heavily on the Hamiltonian reduction formulas. This has allowed us to sidestep several additional features of the theory (such as an explanation of the measure). The holographic dual of bilocals in the Schwarzian are boundary-anchored Wilson lines in JT gravity. OTO-correlation functions of the particle-on-a-group and Schwarzian were determined in terms of crossing Wilson lines in the bulk, giving 6j symbols in the process. For the case of the Schwarzian/JT gravity, it was shown in [25] that these contain the entire gravitational shockwave expansion, including Lyapunov behavior.

Explicitly, we provided a constructive derivation of correlators of boundary-anchored Wilson lines in 2d BF and 2d Yang-Mills, first for compact groups and afterwards for $SL(2, \mathbb{R})$. Since expectation values of boundary-anchored Wilson lines in $SL(2, \mathbb{R})$ YM and BF did not appear before, matching them with the Schwarzian correlators [23] serves a double purpose: besides establishing the holographic dual of Schwarzian correlators, it also verifies the bulk calculation.

In the process, we explained the structural similarity of 2d YM and BF with boundary conditions: the only difference is in the Hamiltonian propagation factor, but the Hilbert space of both theories is identical. Both Hamiltonians are proportional to the Casimir, but in Yang-Mills the propagation scales with the bulk area A , whereas the BF Hamiltonian lives on the boundary and propagation hence scales with the boundary length L . BF theory is obtained by taking $e \rightarrow 0$ in YM, and choosing specific boundary conditions that introduce a boundary action.

In [37], it was established that certain classes of boundary anchored Wilson lines in YM have an interpretation in terms of particle-on-a-group correlators: the mapping is simply $eA_i = L_i$ where A_i is the area of the bulk region touching the boundary segment i . This is made explicit by considering wedge-shaped Wilson line configurations in YM [37]. Likewise, the Schwarzian correlators have an interpretation as wedge-diagrams in constrained $SL(2, \mathbb{R})$ Yang-Mills.

We remarked at various points in section 4 that the matrix elements of the constrained $SL(2, \mathbb{R})$ system are precisely the Liouville wavefunctions, and this means that the resulting integrations are technically identical. This is a generic feature of the Hamiltonian reduction where the Casimir operator explicitly turns into the Liouville minisuperspace Hamiltonian, as reviewed in appendix E.3. This extends to close cousins of Liouville CFT. E.g. the $\mathcal{N} = 1$ $OSp(1|2)$ Casimir operator was diagonalized in [76], leading to the wavefunctions

$$\psi_{k,\pm}(\phi) \sim e^{\phi/2} \left(K_{ik+\frac{1}{2}}(e^\phi) \pm K_{ik-\frac{1}{2}}(e^\phi) \right), \quad (5.1)$$

which can be directly identified with the $\mathcal{N} = 1$ Liouville minisuperspace wavefunctions as determined in [77]. These wavefunctions were used in [23] to determine $\mathcal{N} = 1$ super-Schwarzian correlators. Hence, the $\mathcal{N} = 1$ Schwarzian correlators can be calculated from Wilson lines in constrained $\text{OSp}(1|2)$ BF.

This holds for 2d Toda CFT as well, for which the W_N -symmetry is the pivotal structure. This CFT is expected to contain information on the higher spin Schwarzian systems. E.g. the (Euclidean) higher spin Schwarzian action for the W_3 case is given by [36]:

$$S = -C \int d\tau \left(\frac{f'''}{f'} - \frac{4}{3} \left(\frac{f''}{f'} \right)^2 + \frac{e'''}{e'} - \frac{4}{3} \left(\frac{e''}{e'} \right)^2 - \frac{1}{3} \frac{f'' e''}{f' e'} \right), \quad (5.2)$$

in terms of two time reparametrizations f and e . This would be an interesting system to understand further. In light of our treatment of Hamiltonian reduction, we collect the relevant equations in appendix F to obtain Toda / higher spin Schwarzian from the $\text{SL}(n, \mathbb{R})$ WZW / particle-on-a-group model, with in particular the so-called Whittaker functions playing role both as wavefunctions of the Toda minisuperspace model, and as $\text{SL}(n, \mathbb{R})$ Casimir eigenfunctions [78].

As mentioned in section 2.2, it is possible to consider more general configurations of boundary-anchored Wilson than the ones discussed here, by allowing three or more Wilson lines to end in a bulk vertex. Small gauge invariance requires that these couple to the identity, such that a three-vertex comes with an additional $3j$ -symbol, a four-vertex comes with a sum over two $3j$ -symbols etcetera. The net effect is that a three-vertex in the bulk becomes a $6j$ -symbol in diagrammatic language, a four-vertex becomes a $9j$ -symbol summed over one of the irreps appearing in it i.e. by summing over all intermediate states, etcetera. This opens up the possibility to investigate networks of Wilson lines in the bulk. In 3d CS certain such networks consisting of three-vertices were shown to calculate conformal blocks in 2d WZW [75, 79], and to be related with the OPE as well as with bulk reconstruction using HKLL, where one of the Wilson lines connects the vertex to a local bulk operator [80]. It could be interesting to make explicit the dimensional reduction of this story.

Acknowledgements

The authors thank Nick Bultinck, Nele Callebaut, Luca Iliesiu, Jared Kaplan, Ho Tat Lam, Gustavo Turiaci and Herman Verlinde for several valuable discussions. AB and TM gratefully acknowledge financial support from Research Foundation Flanders (FWO Vlaanderen).

A Knots in BF

The Hamiltonian of BF theory has support only on the boundary and hence all interesting dynamics takes place on the boundary. As discussed in the main text, the interesting

observables are boundary-anchored Wilson lines or boundary bilocals. Aside from this dynamical sector, there is an interesting set of purely topological knot observables that are analogous to the knot expectation values in 3d Chern-Simons [41].

In arbitrary dimensions, BF theory is defined as:

$$S = \frac{k}{4\pi} \int_{\mathcal{M}} \text{Tr} B \wedge F, \quad F = dA + A \wedge A, \quad (\text{A.1})$$

where we omitted the boundary term irrelevant for the purely bulk objects considered here. The interesting bulk operators in this theory are Wilson loops / surfaces associated to both fields A and B , with Wilson lines of the same type commuting and hence uninteresting.

A.1 Punctures

Specifying to 2d, the BF-path integral has two natural classes of observables:

$$\text{Tr}_R \mathcal{P} e^{i \oint A}, \quad \text{Tr}_R e^{i \Phi(x)}, \quad (\text{A.2})$$

representing respectively Wilson loops and punctures on a 2d region of space. For concreteness, we continue with the Abelian case. The generalization to the non-Abelian case is quantitatively not straightforward (requiring knot-theoretic considerations [41]), but the canonical structure of the theory should be similar. The expectation values of these operators calculate their topological linking. Indeed, the path integral with insertions of both types:

$$\int [\mathcal{D}A \mathcal{D}\Phi] e^{i \oint A} e^{i \beta \Phi(x)} e^{i \oint \Phi F} \quad (\text{A.3})$$

leads to the constraint $F = -\beta \delta(x)$, an Aharonov-Bohm vortex of magnetic flux at the location x . This means Wilson lines in A can be freely deformed, as long as no Φ -puncture is crossed. Correlators of this kind are determined by the Gauss intersection number N :

$$\left\langle e^{i \oint A} e^{i \beta \Phi(x)} \right\rangle = e^{i \alpha \beta N}. \quad (\text{A.4})$$

It is instructive to analyze the canonical structure of this model, and reproduce the above topological result from this perspective. Canonical quantization of the 2d BF proceeds in analogy with that of 3d CS [41], by treating A_0 as a Lagrange multiplier:

$$L = \text{Tr} (\Phi \partial_0 A_1 + \partial_1 \Phi A_0 + i \Phi [A_0, A_1]), \quad (\text{A.5})$$

leading to the canonical algebra:

$$\left[A_1^a(x), \Phi^b(y) \right] = \delta^{ab} \delta(x - y), \quad (\text{A.6})$$

with constraint $D_1 \Phi^a = 0$. Enforcing this constraint on physical wavefunctions, using $\Phi^a(x) = -\frac{\delta}{\delta A_1^a(x)}$ leads immediately to what is called the Gauss' law constraint in EM, which in 2d leads to wavefunctionals of only the gauge-covariant Wilson lines.

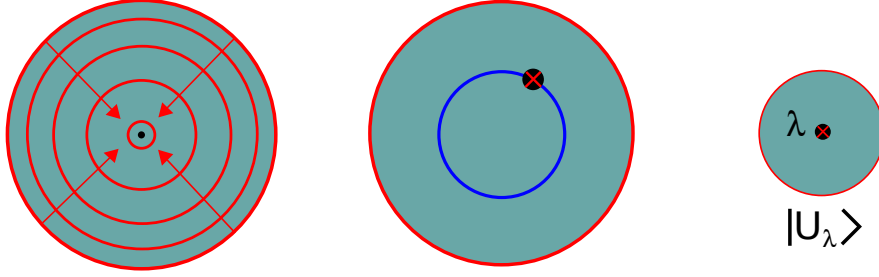


Figure 9. Left: Disk slicing as concentric circles in the character Hilbert basis. Middle: intersecting Wilson line operators. Right: State-operator correspondence associating a fixed holonomy state $|U_\lambda\rangle$ to a local puncture in the representation R .

Choose now a disk and fix the coordinates as $A_0 = A_\rho$ and $A_1 = A_\phi$ in radial quantization of the theory for convenience (Figure 9 left). Defining Wilson loops and punctures as:

$$\mathcal{W}_\alpha = e^{i\alpha \int_0^{2\pi} d\phi A_\phi(x)}, \quad \mathcal{W}_\beta = e^{i\beta \Phi(x)}, \quad (\text{A.7})$$

the canonical algebra (A.6) results in the fundamental “equal-time” exchange algebra:

$$\mathcal{W}_\alpha \mathcal{W}_\beta = e^{i\alpha\beta} \mathcal{W}_\beta \mathcal{W}_\alpha, \quad (\text{A.8})$$

for a circular Wilson loop that intersects the local operator \mathcal{W}_β (Figure 9 middle). In a radially quantized path integral, this is to be read as the cost of moving one Wilson line through a puncture. This contour deforming situation is exactly as happens in 2d CFT. This means that \mathcal{W}_β , as a local operator puncture, changes the holonomy eigenvalue of a state. Indeed, the above algebra implies

$$\mathcal{W}_\alpha \mathcal{W}_\beta |U = \mathbf{1}\rangle = e^{i\alpha\beta} \mathcal{W}_\beta \mathcal{W}_\alpha |U = \mathbf{1}\rangle = e^{i\alpha\beta} \mathcal{W}_\beta |U = \mathbf{1}\rangle, \quad (\text{A.9})$$

such that a holonomy eigenstate is obtained as $\mathcal{W}_\beta |U = \mathbf{1}\rangle = |U = e^{i\beta}\rangle$. We proved this result for the abelian case, but it seems evident that this will hold in the non-abelian case as well: $\text{Tr}_R e^{i\Phi(x)}$ creates a U -eigenstate using the well-known isomorphism between holonomies and irreps in group theory [42]:

$$U_\lambda = e^{-\frac{2\pi}{k}\lambda}, \quad (\text{A.10})$$

for finite weight vector λ and vector of Cartan matrices \mathbf{H} , and $\lambda = \lambda \cdot \mathbf{H}$. This is to be interpreted as a state-operator correspondence of a local irrep λ puncture to a holonomy eigenstate $|U_\lambda\rangle$ that represents a tiny circle around the defect (Figure 9 right). The partition function of BF on a disk with such a holonomy U_λ defect in the interior results in the twisted partition function:

$$\sum_R \dim R \chi_R(U_\lambda) e^{-TH_R}, \quad (\text{A.11})$$

using concentric circle slicing of the disk. As discussed further on in appendix C, this is the $k \rightarrow \infty$ dimensional reduction of the torus path integral χ_λ of 3d Chern-Simons with

a bulk Wilson line in irrep λ inserted along the dimension that is to be reduced, which is dual to a twisted chiral WZW on the torus boundary. This dimensionally reduces to a twisted particle-on-a-group whose partition function matches (A.11). This makes explicit that the puncture in irrep λ is the dimensional reduction of a 3d CS Wilson line in irrep λ .

A disk with n punctures labeled by λ_i and boundary holonomy U results in

$$\sum_R \chi_R(U) (\dim R)^{1-n} \prod_i \chi_R(U_{\lambda_i}) e^{-TH_R}. \quad (\text{A.12})$$

As an additional feature, multiple punctures allow for non-trivial knots in the bulk of Wilson loops encircling the punctures (Figure 10).

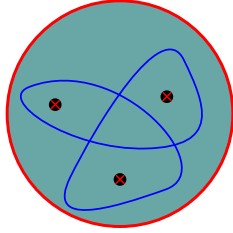


Figure 10. Example of a bulk knot with three local $e^{i\beta\Phi(x)}$ punctures.

As an example, a disk with two punctures $\lambda_{1,2}$ and holonomy U_3 on the outer boundary, is given by:

$$\sum_R \frac{\chi_R(U_{\lambda_1}) \chi_R(U_{\lambda_2}) \chi_R(U_3)}{\dim R} e^{-TH_R}. \quad (\text{A.13})$$

The topological limit $H_R \rightarrow 0$ of this formula is the $k \rightarrow \infty$ limit of the Verlinde formula of the CFT fusion rules:

$$\sum_R \frac{\chi_R(U_{\lambda_1}) \chi_R(U_{\lambda_2}) \chi_R(U_3)}{\dim R} = \lim_{k \rightarrow \infty} \sum_R \frac{S_{\lambda_1 R} S_{\lambda_2 R} S_{\lambda_3 R}}{S_{0R}} = N_{\lambda_1 \lambda_2 \lambda_3}. \quad (\text{A.14})$$

This formula can be inverted, using orthonormality of the character basis, as

$$\frac{\chi_R(U_{\lambda_1}) \chi_R(U_{\lambda_2})}{\dim R} = \int dU_3 N_{\lambda_1 \lambda_2 \lambda_3} \chi_R(U_3), \quad (\text{A.15})$$

which is the Clebsch-Gordan series for the characters.

Equation (A.14) can be seen as the amplitude of the three-holed sphere in BF, which has no physical boundary and hence no boundary Hamiltonian. Again, this is to be compared with the $k \rightarrow \infty$ limit of a configuration in 3d CS where three Wilson lines along S^1 in irreps λ_i are inserted in the path integral on $S^2 \times S^1$.

The disk state with two punctures, denoted as $|U_{\lambda_1 \otimes \lambda_2}\rangle$, can be expanded in the complete basis of holonomy eigenstates, which by the state-operator correspondence (A.10),

can be parametrized by the set of all single punctures on the disk:

$$|U_{\lambda_1 \otimes \lambda_2}\rangle = \int dU_{\lambda_3} \langle U_{\lambda_3} | U_{\lambda_1 \otimes \lambda_2} \rangle |U_{\lambda_3}\rangle \quad (\text{A.16})$$

The overlap amplitude $\langle U_{\lambda_3} | U_{\lambda_1 \otimes \lambda_2} \rangle$ is computed by gluing the two disks together resulting in a three-holed sphere amplitude:

$$\langle U_{\lambda_3} | U_{\lambda_1 \otimes \lambda_2} \rangle = Z_{S^2}(\lambda_1, \lambda_2, \lambda_3) = N_{\lambda_1 \lambda_2 \lambda_3}, \quad (\text{A.17})$$

which by (A.14) is just the fusion coefficient. This is depicted in Figure 11 left. In terms

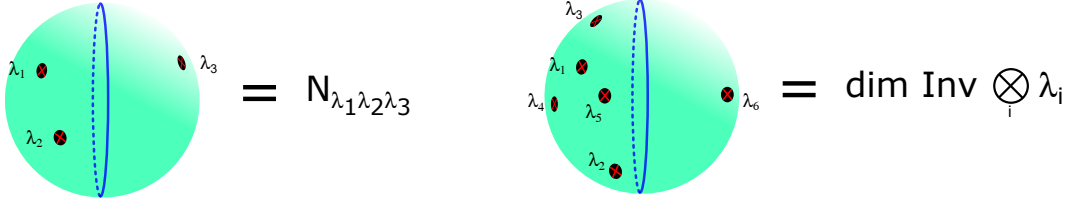


Figure 11. Left: Fusion coefficient as three-holed sphere in BF. Right: Generic n -hole sphere amplitude gives the number of times the identity appears in the tensor product $\otimes_i \lambda_i$.

of correlators, applying $\langle \mathbf{1} | e^{-T\hat{H}}$ to the left of (A.16), allows us to expand a disk with two punctures into a sum over disks with one puncture (Figure 12):

$$Z_{B^1}(\lambda_1, \lambda_2) = \int dU_{\lambda_3} Z_{S^2}(\lambda_1, \lambda_2, \lambda_3) Z_{B^1}(\lambda_3) = \int dU_{\lambda_3} N_{\lambda_1 \lambda_2 \lambda_3} Z_{B^1}(\lambda_3), \quad (\text{A.18})$$

Explicitly, this can also be read off from the formula (A.15). In terms of particle-on-a-group

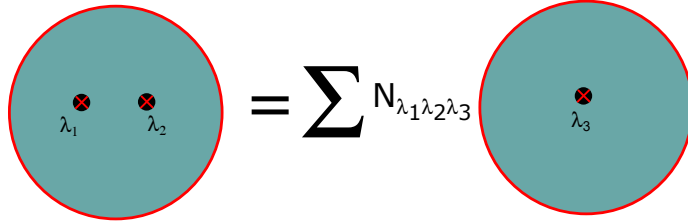


Figure 12. Fusing two Φ -punctures into a single one.

path integrals, using (A.18) the twice-punctured disk amplitude decomposes into a sum of particle-on-a-group amplitudes with twisted boundary conditions:

$$Z_{B^1}(\lambda_1, \lambda_2) = \sum_{\lambda_3} N_{\lambda_1 \lambda_2 \lambda_3} \int [\mathcal{D}g]_{g(\tau+\beta)=U_{\lambda_3}g(\tau)} e^{-S[g]}. \quad (\text{A.19})$$

Alternatively, from the BF path integral with two Φ -insertions (as in (A.3)), integrating out Φ leads to a locally exact 1-form A . When going around the boundary of the disk, it picks up a non-trivial holonomy

$$\text{Tr}_{\lambda_3} \mathcal{P} e^{i \oint A} = U_{\lambda_3} = g(\tau + \beta)g(\tau)^{-1}, \quad (\text{A.20})$$

the value of which is precisely determined by the above Clebsch-Gordan decomposition.

The generalization to a disk with n punctures is straightforward: this can again be decomposed into a sum over disks with one puncture associated with a twisted particle on a group, as:

$$Z_{B^1}(\lambda_1, \lambda_2, \dots, \lambda_n) = \int dU_\lambda Z_{S^2}(\lambda_1, \lambda_2, \dots, \lambda_n, \lambda) Z_{B^1}(\lambda). \quad (\text{A.21})$$

This is illustrated in Figure 11 right. The n -point amplitude on the two sphere is just the number of times the identity appears in the tensor product decomposition $\otimes_i R_i$, or the dimension of the Chern-Simons Hilbert space on $S^2 \times \mathbb{R}$ [41]:

$$Z_{S^2}(\lambda_1, \lambda_2, \dots, \lambda_n) = \dim \mathcal{H}_{S^2}^{CS} = \dim \text{Inv}(\lambda_1 \otimes \lambda_2 \otimes \dots \lambda_n). \quad (\text{A.22})$$

A.2 Diagrammatic Rules

The inclusion of the possibility of punctures in generic amplitudes adds an extra line to the diagrammatic rules of section 2.3:

- Within each region of the disk, labeled by irrep R_i , each puncture λ_j contributes a weight $\frac{\chi_{R_i}(U_{\lambda_j})}{\dim R_i}$.

The denominator stems from the fact that each puncture augments the Euler characteristic of the disk by one. These rules allows for the calculation of a generic knot configuration in BF, possibly including boundary-anchored Wilson lines.

Alternatively, one could calculate a given amplitude by stepwise simplifying it using the appropriate exchange algebra to pull non-Abelian Wilson lines through punctures, and eventually reducing the multiple punctures to a single puncture as explained above. One is left with a sum over twisted particle on a group diagrams with possibly boundary-anchored Wilson lines. The latter can then be calculated explicitly as explained in the main text.

A.3 Wilson Loop Crossings

The canonical algebra of BF (A.6) shows that Wilson loops commute, meaning that they can be pulled through one another at will, and configurations including extensive crossings of Wilson lines can be greatly simplified before embarking on the calculation. Some examples of crossings that can be undone are drawn in Figure 13.

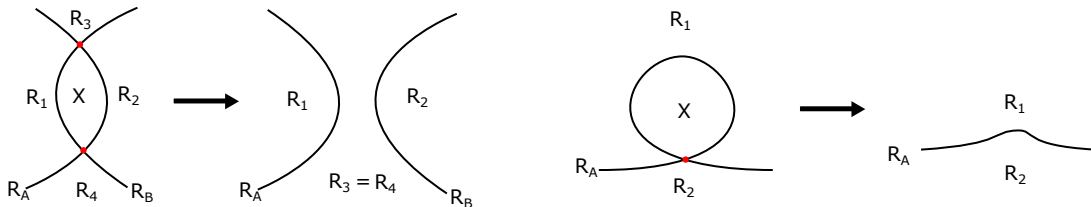


Figure 13. Wilson line crossings that can be undone. Left: Double crossing of two lines. Right: Self-crossing of a single line.

It is amusing to see these moves explicitly in formulas as properties of $6j$ -symbols. More explicitly, undoing one double crossing (Figure 13 left) is achieved by using the identity

$$\dim R \sum_X \dim X \left\{ \begin{matrix} R_A & R_1 & R_3 \\ R_B & R_2 & X \end{matrix} \right\} \left\{ \begin{matrix} R_A & R_1 & R_4 \\ R_B & R_2 & X \end{matrix} \right\} = \delta_{R_3 R_4}. \quad (\text{A.23})$$

Similarly, a self-crossing of a Wilson line (Figure 13 right) in the bulk can be undone by:

$$\sum_X \dim X \left\{ \begin{matrix} R_A & R_1 & R_2 \\ R_A & R_1 & X \end{matrix} \right\} = 1. \quad (\text{A.24})$$

Furthermore, a single bulk Wilson loop produces just an overall degeneracy factor $\dim R$. Indeed, the disk amplitude of a bulk Wilson line is obtained by taking the trace in (2.19):

$$\int dg \chi_{R_1}(g) \chi_{R_2}(g) \chi_{R_3}(g) = N_{R_1 R_2 R_3}, \quad (\text{A.25})$$

such that

$$\langle \mathcal{W}_R \rangle = \sum_{R_1, R_2} \dim R_2 N_{R_1 R_2 R} e^{-\beta H(R_1)} = \dim R \sum_{R_1} \dim R_1 e^{-\beta H(R_1)} = \dim R \langle \mathbf{1} \rangle, \quad (\text{A.26})$$

where we used the identity

$$\sum_{R_2} \dim R_2 N_{R_1 R_2 R} = \dim R \dim R_1. \quad (\text{A.27})$$

Thus, Wilson lines in the bulk that do not enclose punctures produce just overall prefactors in amplitude and are not interesting observables to consider. For the purpose of completeness let us mention that such Wilson lines can be calculated from the particle-on-a-group perspective by taking the coincident limit of both endpoints of a single boundary-anchored Wilson line.

B Some Elementary Properties of Representation Matrices

We collect some properties we need on integrals of representation matrices $R_{mn}(g) \equiv \langle m | g | n \rangle$. Schur's orthogonality relation is given by:

$$\int dg R_{ab}(g) R'_{cd}(g^{-1}) = \frac{\delta_{RR'}}{\dim R} \delta_{ad} \delta_{bc}, \quad (\text{B.1})$$

also called the grand orthogonality theorem. The completeness relation

$$\sum_{R, m, n} \dim R R_{mn}(g_1) R_{nm}(g_2^{-1}) = \delta(g_1 - g_2), \quad (\text{B.2})$$

with $\delta(g)$ defined in the Haar measure, is guaranteed by the Peter-Weyl theorem. These two properties combined allow us to write a complete normalized set of basis states $\{|R, mn\rangle\}$, whose wavefunctions are just the representation matrices:

$$\langle g | R, mn \rangle \equiv \sqrt{\dim R} R_{mn}(g), \quad \langle R, mn | g \rangle \equiv \sqrt{\dim R} R_{nm}(g^{-1}), \quad (\text{B.3})$$

with orthonormality $\langle R_1, m_1, n_1 | R_2, m_2, n_2 \rangle = \delta(R_1 - R_2)\delta(m_1 - m_2)\delta(n_1 - n_2)$ and completeness $\sum_{R,m,n} |R, mn\rangle \langle R, mn| = \mathbf{1}$ following from (B.1) and (B.2). Note that $\langle R, mn | g \rangle = \langle g | R, mn \rangle$ implies $R_{nm}(g^{-1}) = \overline{R_{mn}(g)}$, implying only unitary representations are included.

The Kronecker tensor product of two representation matrices, can be expanded in a Clebsch-Gordan series as:

$$\begin{aligned} R_{1m_1n_1}(g)R_{2m_2n_2}(g) &\equiv \langle R_1, m_1 | \otimes \langle R_2, m_2 | g | R_1, n_1 \rangle \otimes | R_2, n_2 \rangle \\ &= \sum_{R_3, \bar{R}_3, m_3, n_3} C_{R_1m_1, R_2m_2}^{R_3m_3} C_{R_1n_1, R_2n_2}^{\bar{R}_3n_3} \langle R_3, m_3 | g | \bar{R}_3, n_3 \rangle \\ &= \sum_{R_3, m_3, n_3} C_{R_1m_1, R_2m_2}^{R_3m_3} C_{R_1n_1, R_2n_2}^{R_3n_3} R_{3, m_3 n_3}(g), \end{aligned} \quad (\text{B.4})$$

a property well-known for the Wigner D-functions for SU(2). Hence, we can write for the group integral of three representation matrices (using (B.1)):

$$\begin{aligned} &\int dg R_{1, m_1 n_1}(g) R_{2, m_2 n_2}(g) R_{3, n_3 m_3}(g^{-1}) \\ &= \sum_{R, m, n} C_{R_1m_1, R_2m_2}^{Rm} C_{R_1n_1, R_2n_2}^{Rn} \int dg R_{mn}(g) R_{3, n_3 m_3}(g^{-1}) \\ &= \frac{C_{R_1m_1, R_2m_2}^{R_3m_3} C_{R_1n_1, R_2n_2}^{R_3n_3}}{\dim R_3} \\ &= (-)^{R_2 - R_1 + m_3} (-)^{R_2 - R_1 + n_3} \begin{pmatrix} R_1 & R_2 & R_3 \\ m_1 & m_2 & -m_3 \end{pmatrix} \begin{pmatrix} R_1 & R_2 & R_3 \\ n_1 & n_2 & -n_3 \end{pmatrix}. \end{aligned} \quad (\text{B.5})$$

We need this property in the main text. The $3j$ -symbols satisfy the orthogonality property:

$$\dim R_3 \sum_{m_1, m_2} \begin{pmatrix} R_1 & R_2 & R_3 \\ m_1 & m_2 & m_3 \end{pmatrix} \begin{pmatrix} R_1 & R_2 & \tilde{R}_3 \\ m_1 & m_2 & \tilde{m}_3 \end{pmatrix} = \delta_{R_3 \tilde{R}_3} \delta_{m_3 \tilde{m}_3}. \quad (\text{B.6})$$

Throughout this work, we will absorb all minus signs in (B.5) into the definition of the $3j$ -symbols to streamline the notation.

C WZW and Particle-on-a-group

We provide some details on how the particle-on-a-group theory arises from 2d Wess-Zumino-Witten (WZW) CFT. The appearance of the particle-on-a-group theory from WZW is ubiquitous. We discuss the $k \rightarrow \infty$ dimensional reduction on a torus of both a chiral and a non-chiral WZW, resulting in the same theory.

C.1 Non-Chiral WZW

The non-chiral WZW model

$$S_{\text{WZW}} = \frac{k}{16\pi} \int d^2z \text{Tr}(g^{-1} \partial g g^{-1} \bar{\partial} g) + k\Gamma_{\text{WZ}}, \quad (\text{C.1})$$

with Γ_{WZ} the Wess-Zumino term and $g(z, \bar{z}) \in G$, defined on a torus worldsheet, leads to the thermal particle-on-a-group model after taking a double scaling limit where one of the cycles of the torus goes to zero, and the level $k \rightarrow +\infty$ keeping their product fixed. This procedure effectively sets $\partial, \bar{\partial} \rightarrow \partial_t$ and removes the Wess-Zumino term. The action (C.1) almost trivially reduces to the action of quantum mechanics on the G -manifold.

The WZW partition function is the diagonal modular invariant which contains a sum over all integrable representations \hat{R} of $\hat{\mathfrak{g}}$. Taking the double-scaling limit directly in the growing channel, leads to:

$$Z(\tau) = \sum_{\hat{R}} |\chi_{\hat{R}}(\tau)|^2 \xrightarrow{\tau_2 \rightarrow +\infty, k \rightarrow \infty} \sum_R \left| \dim \mathbb{R} e^{-\frac{\beta}{2} H_R} \right|^2, \quad \beta = 2\pi \frac{\tau_2}{k + g^\vee}, \quad (\text{C.2})$$

because the characters in this channel reduces to the zero-grade sector in the double-scaling limit [23]. States of WZW are labeled by $|R, m\bar{m}, n\bar{n}\rangle$. The double-scaling limit projects on the zero-grade sector in the closed channel resulting in the particle-on-a-group spectrum $|R, m\bar{m}\rangle$. The partition function (C.2) should be read as constructed from this Hilbert space $|R, m\bar{m}\rangle$ with unity degeneracy.

Note that correlation functions of local WZW fields reduce in the limit to *local* particle-on-a-group operators, and 3d Wilson lines in CS reduce to 2d Wilson lines in BF, both dual to bilocals. A priori without bulk knowledge, the resulting particle-on-a-group operators need not be associated with any bulk Wilson line. In the language of the particle-on-a-group calculation performed in Appendix D, this means that one could consider operators whose indices are not contracted. These operators are however not invariant under the global G gauge redundancy and are hence not observables. Instead these operators are G -covariant. Such operators were studied in the Schwarzian model in [23].

C.2 Coadjoint Orbit

The chiral WZW model (CWZW) associated with an integrable representation λ has action:

$$S_{\text{CWZW}}^\lambda = \frac{k}{4\pi} \int dt d\phi \text{Tr}(g^{-1} \partial_\phi g g^{-1} (\partial_t - \partial_\phi) g) + k \Gamma_{\text{WZ}} + \text{Tr}(\lambda g^{-1} (\partial_t - \partial_\phi) g), \quad (\text{C.3})$$

where $\lambda = \lambda \cdot \mathbf{H}$, with \mathbf{H} the Cartan representation matrices. This is just the Kac-Moody coadjoint orbit action of the element λ .²¹ It is found as the boundary action of Chern-Simons with a Wilson line in representation λ in the bulk, stretched in the time-direction. The path integral of this action yields the character χ_λ in the time-direction. The untwisted particle-on-a-group action is obtained by dimensional reduction of the vacuum $\lambda = 0$ coadjoint orbit along the t -direction.

²¹This is related to the more familiar Kirillov-Kostant formula for a single character of the group G , computed as a path-integral on the coadjoint orbit of λ by restricting (C.3) to the angular ϕ -zero-mode:

$$S_{\text{CWZW}}^\lambda \rightarrow \int dt \text{Tr}(\lambda g^{-1} \partial_t g). \quad (\text{C.4})$$

Additionally a term $\text{Tr}\lambda^2$ could be added, giving the Casimir as Hamiltonian in the character.

The partition function is the double scaling limit of the vacuum character χ_0 . This is most conveniently evaluated in the closed channel described above, for which in the double scaling limit the characters become traces over the zero grade sector only. The vacuum character decomposes into closed channel characters as:

$$\begin{aligned} \chi_0(it) &= \text{Tr} q^{L_0} = \langle 0 | e^{-\frac{\pi}{t}(L_0 + \bar{L}_0)} | 0 \rangle = \sum_{\hat{R}} S_{0\hat{R}} \chi_{\hat{R}}(i/t), \quad q = e^{-2\pi t} \\ &\xrightarrow{t \rightarrow 0, k \rightarrow \infty} \sum_R \dim R \left(\dim \text{Re}^{-\beta H_R} \right), \quad \beta t = \frac{2\pi}{k + g^\vee}. \end{aligned} \quad (\text{C.5})$$

The second equality of the first line illustrates that one should think of the Hilbert space again as a ‘‘closed’’ sector $|R, m\bar{m}\rangle$. Ordinarily, this makes no difference, as the brane boundary states project on the chiral sector anyway. But when inserting operators this becomes important. We have seen in the main text that the second \bar{m} label in intermediate channels cannot be dropped for spinning operator insertions $\mathcal{O}_{R, M\bar{M}}$ with $M \neq \bar{M}$.

For a generic weight λ , dimensional reduction of (C.3) to the t -zero-mode, with $k \int dt = C$ held fixed, leads to:

$$S_{\text{CWZW}}^\lambda \rightarrow -\frac{C}{4\pi} \int d\phi \text{Tr}(g^{-1} \partial_\phi g)^2 - \text{Tr}(\tilde{\lambda} g^{-1} \partial_\phi g). \quad (\text{C.6})$$

To obtain a finite second term, one is to consider weights scaling as $\lambda \sim k \rightarrow \infty$, resulting in a finite $\tilde{\lambda} = \lambda \int dt$. This particular scaling leads, up to some irrelevant multiplicative factors, to [45, 46]:

$$S_{\lambda R} \rightarrow \chi_R(U_\lambda), \quad (\text{C.7})$$

with $R \sim k^0$ and $\lambda \sim k^1$. The holonomy U_λ is determined from the irrep λ by (A.10). The scaling $\lambda \sim k$ results indeed in a finite holonomy in the double-scaling limit. The double-scaling limit of the $\hat{\lambda}$ -coadjoint orbit hence becomes:

$$\chi_{\hat{\lambda}} = \sum_R S_{\hat{\lambda}R} \chi(-1/\tau) \rightarrow \sum_R \chi_R(U_\lambda) \left(\dim \text{Re}^{-\beta H_R} \right). \quad (\text{C.8})$$

Alternatively, as shown in [81], the second term in the action (C.6) can be absorbed into the first using a new field g that has twisted boundary conditions $g(\phi + \beta) = U_\lambda g(\phi)$, and the resulting twisted particle-on-a-group computation indeed gives precisely this result (C.8).

A non-chiral WZW model can be decomposed into two chiral WZW models, see e.g. [82]. The classical solution of the equations of motion of (C.1) is given by:

$$g(x^+, x^-) = g_L(x^+) g_R^{-1}(x^-), \quad g_{L/R}(x^\pm + 2\pi) = g_{L/R}(x^\pm) U, \quad (\text{C.9})$$

for holonomy $U \in G$. The phase space \mathcal{M} consists of degrees of freedom contained in g_{LR} and U , and using the association of a irrep λ with U (A.10), it can be written as

$$\mathcal{M} = \sum_{\hat{\lambda}} \mathcal{M}_\lambda = \sum_{\hat{\lambda}} \frac{LG_\lambda \times LG_\lambda}{G}. \quad (\text{C.10})$$

The non-chiral WZW path integral, is written in phase space as

$$\int_{\mathcal{M}} [\mathcal{D}g\mathcal{D}\pi_g] e^{-\frac{k}{16\pi} \int d^2z \text{Tr}[\pi_g g^{-1} \dot{g} - \frac{1}{2}(\pi_g^2 + (g^{-1} \dot{g}')^2)] + k\Gamma_{\text{WZ}}}. \quad (\text{C.11})$$

Changing field variables from (g, π_g) into (g_L, g_R) as

$$g = g_L g_R^{-1}, \quad \pi_g = g_R g_L^{-1} \partial_\phi g_L g_R^{-1} + \partial_\phi g_R g_R^{-1}, \quad (\text{C.12})$$

including an integral over the twist U , one finds the action reduces to a sum of two chiral WZW models:

$$\sum_{\hat{\lambda}} \int_{\mathcal{M}_{\hat{\lambda}}} [\mathcal{D}g_L] [\mathcal{D}g_R] e^{-S_{\text{CWZW}}^{\hat{\lambda}}[g_L] - S_{\text{CWZW}}^{\hat{\lambda}}[g_R]}, \quad (\text{C.13})$$

with $S_{\text{CWZW}}^{\hat{\lambda}}[g]$ given by (C.3). Note that when considering the non-chiral theory between branes (take e.g. one vacuum brane and one arbitrary brane), the additional boundary conditions enforce $g_L = g_R$ and fix $U_{\hat{\lambda}}$ in terms of the specific boundary state $|\hat{\lambda}\rangle$. In this case, the transformation (C.12) then leads to a single chiral WZW model, with phase space $LG_{\hat{\lambda}}/G$, a perspective made explicit for the Schwarzian theory in [24].

C.3 Branes

The calculations in [24] relating WZW to particle-on-a-group considered non-chiral WZW between vacuum branes as ancestor of particle-on-a-group (Figure 14). This is by definition the chiral WZW model described above. In the closed channel, a vacuum brane

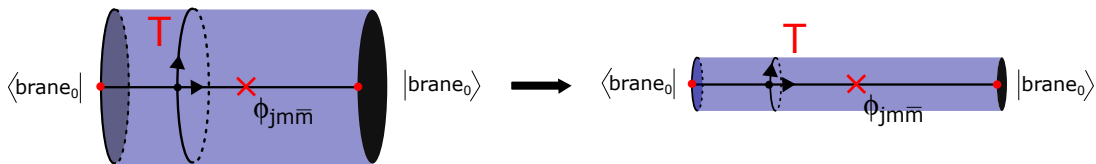


Figure 14. Left: Cylinder amplitude in WZW between vacuum branes $|\text{brane}_0\rangle$. Right: Double scaling limit where the circumference of the cylinder $T \rightarrow 0$, as $k \rightarrow \infty$ keeping the product fixed $kT \sim C$. A local WZW puncture gives a bilocal operator in the dimensionally reduced particle-on-a-group model.

is characterized by an initial (or final) state $|0\rangle = \sum_{\hat{\lambda}} \sqrt{S_{0\hat{\lambda}}} |\hat{\lambda}\rangle$ with $|\hat{\lambda}\rangle$ the Ishibashi state. In the double-scaling limit, the Ishibashi state reduces to a sum over diagonal states $|\hat{\lambda}\rangle = \sum_m |\lambda, mm\rangle$. Crucially, this construction in no way alters the Hilbert space of the theory which is a local construction independent of any branes.

Changing a single brane boundary state from $|0\rangle$ into $|\lambda\rangle$, leads to the character $\chi_{\hat{\lambda}}$. The fact that the dimensional reduction of this configuration does not yield a nice thermal partition function (C.8) resonates with the fact that in the Schwarzian theory, other branes do not give a well-defined 1d thermal system [23, 24].

Local operators in non-chiral WZW between branes are in the double scaling limit taken to bilocal operator insertions in the particle-on-a-group model [24]:²²

$$\mathcal{O}_{j,m\bar{m}}(\tau_1, \tau_2) = R_{j,m\bar{m}}(g(\tau_2)g^{-1}(\tau_1)). \quad (\text{C.14})$$

Correlators of n of these bilocals were calculated as the limit of n -point functions of primary operators in WZW. Upon expanding the vacuum brane into Ishibashi states, and introducing complete sets of states between each local WZW insertion, such a computation is reduced to a number of matrix elements of primary operators. Using group theory, these three-point functions can then be directly computed in coordinate space as:

$$\langle j_1, m_1, \bar{m}_1 | \mathcal{O}_{j,m\bar{m}} | j_2, m_2, \bar{m}_2 \rangle = \int dg \langle j_1, m_1, \bar{m}_1 | g \rangle R_{j,m\bar{m}}(g) \langle g | j_2, m_2, \bar{m}_2 \rangle, \quad (\text{C.15})$$

where we introduced a completeness relation. Using expressions (2.5) and (2.19), the wavefunctions can be written out and the integral performed:²³

$$\langle j_1, m_1, \bar{m}_1 | \mathcal{O}_{j,m\bar{m}} | j_2, m_2, \bar{m}_2 \rangle = \sqrt{\dim j_1} \sqrt{\dim j_2} \begin{pmatrix} j_1 & j & j_2 \\ m_1 & m & m_2 \end{pmatrix} \begin{pmatrix} j_1 & j & j_2 \\ \bar{m}_1 & \bar{m} & \bar{m}_2 \end{pmatrix}. \quad (\text{C.16})$$

The derivation of this relation provides a faster route towards the $3j$ -symbol decomposition (2.35) of particle-on-a-group correlators than the one presented in [23], where a 2d argument in terms of the Wigner-Eckart theorem was given.

D Correlation Functions in Particle-on-a-group

In the bulk text we have calculated particle-on-a-group correlators using holography. In [24], these were calculated using the embedding of particle-on-a-group in WZW. In this appendix we provide details of the third way of calculating these correlation functions: by means of a direct calculation in particle-on-a-group.

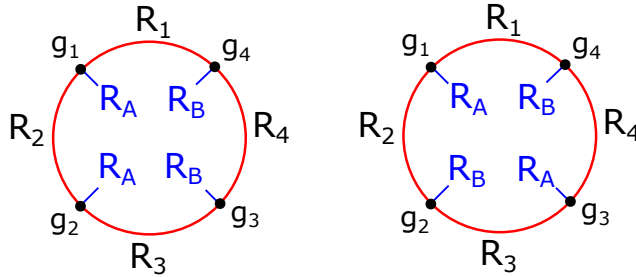


Figure 15. Left: Four-point correlator for the thermal particle-on-a-group model. Right: Four-point correlator with crossed bilocal operators.

²²Actually one should think of the higher dimensional local operators as local in ϕ but smeared in t , because only the zero-grade operators survive the double scaling.

²³In [24], only spinless operators were considered, effectively restricting all sums to the diagonal sector $m_i = \bar{m}_i$. We present the general situation here.

Using that the bilocal operators are of the form:

$$\begin{aligned}\mathcal{W}_{R_A, m_A \bar{m}_A} &= R_A(g_2)_{m_A \alpha} R_A(g_1^{-1})_{\alpha \bar{m}_A}, \\ \mathcal{W}_{R_B, m_B \bar{m}_B} &= R_B(g_4)_{m_B \beta} R_B(g_3^{-1})_{\beta \bar{m}_B},\end{aligned}\tag{D.1}$$

the time-ordered finite-temperature correlator (Figure 15 left) is computed as

$$\text{Tr} \left[e^{-\beta H} R_B(\hat{g}_4)_{m_B \beta} R_B(\hat{g}_3^{-1})_{\beta \bar{m}_B} R_A(\hat{g}_2)_{m_A \alpha} R_A(\hat{g}_1^{-1})_{\alpha \bar{m}_A} \right].\tag{D.2}$$

Expanding in coordinate space, one obtains

$$\begin{aligned}& \sum_{\alpha, \beta} \int dg_i \langle g_1 | e^{-T_4 H} | g_4 \rangle R_B(g_4)_{m_B \beta} \langle g_4 | e^{-T_3 H} | g_3 \rangle \\ & R_B(g_3^{-1})_{\beta \bar{m}_B} \langle g_3 | e^{-T_2 H} | g_2 \rangle R_A(g_2)_{m_A \alpha} \langle g_2 | e^{-T_1 H} | g_1 \rangle R_A(g_1^{-1})_{\alpha \bar{m}_A}\end{aligned}\tag{D.3}$$

Introducing four complete sets of states to compute each of the four matrix elements, from right to left denoted as $|R_i, m_i \bar{m}_i\rangle$, $i = 1, 2, 3, 4$, one can write

$$\begin{aligned}& \sum_{\alpha, \beta, R_i, m_i \bar{m}_i} \int dg_i \dim R_i e^{-T_4 \mathcal{C}_4} e^{-T_3 \mathcal{C}_3} e^{-T_2 \mathcal{C}_2} e^{-T_1 \mathcal{C}_1} \\ & \times R_4(g_1)_{m_4 \bar{m}_4} R_4(g_4^{-1})_{\bar{m}_4 m_4} R_B(g_4)_{m_B \beta} R_3(g_4)_{m_3 \bar{m}_3} R_3(g_3^{-1})_{\bar{m}_3 m_3} R_B(g_3^{-1})_{\beta \bar{m}_B} \\ & \times R_2(g_3)_{m_2 \bar{m}_2} R_2(g_2^{-1})_{\bar{m}_2 m_2} R_A(g_2)_{m_A \alpha} \langle g_2 | R_1(g_2)_{m_1 \bar{m}_1} R_1(g_1^{-1})_{\bar{m}_1 m_1} R_A(g_1^{-1})_{\alpha \bar{m}_A},\end{aligned}\tag{D.4}$$

which gives

$$\begin{aligned}& \sum_{\alpha, \beta, R_i, m_i \bar{m}_i} \dim R_i e^{-T_4 \mathcal{C}_4} e^{-T_3 \mathcal{C}_3} e^{-T_2 \mathcal{C}_2} e^{-T_1 \mathcal{C}_1} \\ & \times \begin{pmatrix} R_4 & R_1 & R_A \\ m_4 & m_1 & m_A \end{pmatrix} \begin{pmatrix} R_4 & R_1 & R_A \\ \bar{m}_4 & \bar{m}_1 & \alpha \end{pmatrix} \begin{pmatrix} R_3 & R_4 & R_B \\ m_3 & m_4 & \bar{m}_B \end{pmatrix} \begin{pmatrix} R_3 & R_4 & R_B \\ \bar{m}_3 & \bar{m}_4 & \beta \end{pmatrix} \\ & \times \begin{pmatrix} R_2 & R_3 & R_B \\ m_2 & m_3 & m_B \end{pmatrix} \begin{pmatrix} R_2 & R_3 & R_B \\ \bar{m}_2 & \bar{m}_3 & \beta \end{pmatrix} \begin{pmatrix} R_1 & R_2 & R_A \\ m_1 & m_2 & \bar{m}_A \end{pmatrix} \begin{pmatrix} R_1 & R_2 & R_A \\ \bar{m}_1 & \bar{m}_2 & \alpha \end{pmatrix} \\ & = \sum_{R_1, R_2, R_3} \dim R_i e^{-T_4 \mathcal{C}_4} e^{-T_3 \mathcal{C}_3} e^{-T_2 \mathcal{C}_2} e^{-T_1 \mathcal{C}_1} \\ & \times \sum_{m_i} \begin{pmatrix} R_2 & R_1 & R_A \\ m_4 & m_1 & m_A \end{pmatrix} \begin{pmatrix} R_3 & R_2 & R_B \\ m_3 & m_4 & \bar{m}_B \end{pmatrix} \begin{pmatrix} R_2 & R_3 & R_B \\ m_2 & m_3 & m_B \end{pmatrix} \begin{pmatrix} R_1 & R_2 & R_A \\ m_1 & m_2 & \bar{m}_A \end{pmatrix},\end{aligned}\tag{D.5}$$

where we used (B.6) to evaluate several summations, reproducing precisely the time-ordered four-point correlator.

This procedure can be extended to the OTO (or crossed) computation (Figure 15 right) as we now demonstrate. The crossed correlator is computed in the particle-on-a-group model as

$$\text{Tr} \left[e^{-\beta H} R_B(\hat{g}_4)_{m_B \beta} R_A(\hat{g}_3)_{m_A \alpha} R_B(\hat{g}_2^{-1})_{\beta \bar{m}_B} R_A(\hat{g}_1^{-1})_{\alpha \bar{m}_A} \right].\tag{D.6}$$

The index contractions contain all the information on the topological crossing that happens in the bulk. Expanding in coordinate space, one obtains

$$\sum_{\alpha,\beta} \int dg_i \langle g_1 | e^{-T_4 H} | g_4 \rangle R_B(g_4)_{m_B \beta} \langle g_4 | e^{-T_3 H} | g_3 \rangle R_A(g_3)_{m_A \alpha} \langle g_3 | e^{-T_2 H} | g_2 \rangle R_B(g_2^{-1})_{\beta \bar{m}_B} \langle g_2 | e^{-T_1 H} | g_1 \rangle R_A(g_1^{-1})_{\alpha \bar{m}_A}. \quad (\text{D.7})$$

Introducing again four complete sets of states to compute each of the four matrix elements, from right to left denoted as $|R_i, m_i \bar{m}_i\rangle$, $i = 1, 2, 3, 4$, one can write

$$\begin{aligned} \sum_{\alpha,\beta,R_i,m_i,\bar{m}_i} \int dg_i \dim R_i e^{-T_4 \mathcal{C}_4} e^{-T_3 \mathcal{C}_3} e^{-T_2 \mathcal{C}_2} e^{-T_1 \mathcal{C}_1} \\ \times R_4(g_1)_{m_4 \bar{m}_4} R_4(g_4^{-1})_{\bar{m}_4 m_4} R_B(g_4)_{m_B \beta} R_3(g_4)_{m_3 \bar{m}_3} R_3(g_3^{-1})_{\bar{m}_3 m_3} R_A(g_3)_{m_A \alpha} \\ \times R_2(g_3)_{m_2 \bar{m}_2} R_2(g_2^{-1})_{\bar{m}_2 m_2} R_B(g_2^{-1})_{\beta \bar{m}_B} R_1(g_2)_{m_1 \bar{m}_1} R_1(g_1^{-1})_{\bar{m}_1 m_1} R_A(g_1^{-1})_{\alpha \bar{m}_A}, \end{aligned} \quad (\text{D.8})$$

which can be computed as

$$\begin{aligned} \sum_{\alpha,\beta,R_i,m_i,\bar{m}_i} \dim R_i e^{-T_4 \mathcal{C}_4} e^{-T_3 \mathcal{C}_3} e^{-T_2 \mathcal{C}_2} e^{-T_1 \mathcal{C}_1} \\ \times \begin{pmatrix} R_4 & R_1 & R_A \\ m_4 & m_1 & \bar{m}_A \end{pmatrix} \begin{pmatrix} R_4 & R_1 & R_A \\ \bar{m}_4 & \bar{m}_1 & \alpha \end{pmatrix} \begin{pmatrix} R_3 & R_4 & R_B \\ m_3 & m_4 & m_B \end{pmatrix} \begin{pmatrix} R_3 & R_4 & R_B \\ \bar{m}_3 & \bar{m}_4 & \beta \end{pmatrix} \\ \times \begin{pmatrix} R_2 & R_3 & R_A \\ m_2 & m_3 & m_A \end{pmatrix} \begin{pmatrix} R_2 & R_3 & R_A \\ \bar{m}_2 & \bar{m}_3 & \alpha \end{pmatrix} \begin{pmatrix} R_1 & R_2 & R_B \\ m_1 & m_2 & \bar{m}_B \end{pmatrix} \begin{pmatrix} R_1 & R_2 & R_B \\ \bar{m}_1 & \bar{m}_2 & \beta \end{pmatrix} \\ = \sum_{R_i,m_i} \dim R_i e^{-T_4 \mathcal{C}_4} e^{-T_3 \mathcal{C}_3} e^{-T_2 \mathcal{C}_2} e^{-T_1 \mathcal{C}_1} \begin{Bmatrix} R_B & R_1 & R_4 \\ R_A & R_3 & R_2 \end{Bmatrix} \\ \times \begin{pmatrix} R_4 & R_1 & R_A \\ m_4 & m_1 & \bar{m}_A \end{pmatrix} \begin{pmatrix} R_3 & R_4 & R_B \\ m_3 & m_4 & m_B \end{pmatrix} \begin{pmatrix} R_2 & R_3 & R_A \\ m_2 & m_3 & m_A \end{pmatrix} \begin{pmatrix} R_1 & R_2 & R_B \\ m_1 & m_2 & \bar{m}_B \end{pmatrix}, \end{aligned} \quad (\text{D.9})$$

reproducing precisely the crossed four-point correlator.

E Representation Theory of $\text{SL}(2, \mathbb{R})$ in the Parabolic Basis

As the representation theory of $\text{SL}(2, \mathbb{R})$ in the parabolic basis is less widespread, we write down the relevant formulas here and apply them to the constrained system. Much of the material presented here can be found in [57, 64].

E.1 Parabolic Basis

Parametrizing an $\text{SL}(2, \mathbb{R})$ matrix as

$$\begin{pmatrix} a & b \\ c & d \end{pmatrix}, \quad ad - bc = 1, \quad (\text{E.1})$$

a representation is obtained by associating the group transformation

$$f_j(x) \rightarrow (g \cdot f_j)(x) = |bx + d|^{2j} f_j\left(\frac{ax + c}{bx + d}\right), \quad (\text{E.2})$$

to the set of functions on the real line $f_j(x)$, with the definition of the matrix elements as

$$\langle f_1 | g | f_2 \rangle \equiv \int dx f_1(x) (g \cdot f_2)(x). \quad (\text{E.3})$$

This defines a representation of the group with label j , since composing group transformations works as it should:

$$\begin{aligned} \langle f_1 | g_1 g_2 | f_2 \rangle &\equiv \int dx f_1(x) (g_1 g_2 \cdot f_2)(x), & g_i &= \begin{pmatrix} a_i & b_i \\ c_i & d_i \end{pmatrix}, \\ &= \int dx f_1(x) g_1 \cdot \left(|b_2 x + d_2|^{2j} f_2 \frac{a_2 x + c_2}{b_2 x + d_2} \right) \\ &= \int dx f_1(x) |bx + d|^{2j} f_2\left(\frac{ax + c}{bx + d}\right), & g_1 g_2 &= \begin{pmatrix} a & b \\ c & d \end{pmatrix}. \end{aligned} \quad (\text{E.4})$$

Simple algebra demonstrates that one can define the adjoint action of g by the formula:

$$\langle f_1 | g | f_2 \rangle = \int dx f_1(x) (g \cdot f_2)(x) \equiv \int dx (g^\dagger \cdot f_1(x)) f_2(x), \quad (\text{E.5})$$

where hence

$$g^\dagger \cdot f_j(x) = |-bx + a|^{-2j-2} f_j\left(\frac{dx - c}{-bx + a}\right), \quad (\text{E.6})$$

which can be viewed as evaluating f_j on the inverse group element g^{-1} .

The $\mathfrak{sl}(2, \mathbb{R})$ algebra generators are defined as the traceless matrices:

$$J^+ = \begin{pmatrix} 0 & -i \\ 0 & 0 \end{pmatrix}, \quad J^- = \begin{pmatrix} 0 & 0 \\ -i & 0 \end{pmatrix}, \quad J^0 = \frac{1}{2} \begin{pmatrix} i & 0 \\ 0 & -i \end{pmatrix}, \quad (\text{E.7})$$

satisfying the algebra:

$$[J^0, J^\pm] = \pm i J^\pm, \quad [J^+, J^-] = 2i J^0 \quad (\text{E.8})$$

Studying the group transformation (E.2) infinitesimally, using $g = \mathbf{1} + i\epsilon_a J^a$, leads to the Borel-Weil realization of the $\mathfrak{sl}(2, \mathbb{R})$ algebra:

$$\begin{aligned} i\hat{J}^- &= \partial_x, \\ i\hat{J}^0 &= -x\partial_x + j, \\ i\hat{J}^+ &= -x^2\partial_x + 2jx, \end{aligned} \quad (\text{E.9})$$

satisfying the same relations (E.8). The Casimir associated to this representation j computed in this realization equals $\mathcal{C} = (\hat{J}^0)^2 + \frac{1}{2} (\hat{J}^+ \hat{J}^- + \hat{J}^- \hat{J}^+) = j(j+1)$, and demonstrates that (E.2) indeed constructs a spin- j representation.

In the parabolic basis, we choose to diagonalize the subgroup:

$$\mathbf{h}_- = \begin{pmatrix} 1 & 0 \\ t & 1 \end{pmatrix} = \exp itJ^-, \quad t \in \mathbb{R}. \quad (\text{E.10})$$

A basis of the representation is then formed by the plane waves $f_{j\nu}(x) = e^{i\nu x}$, which indeed diagonalize \mathbf{h}_- as

$$\mathbf{h}_- \cdot f_{j\nu}(x) = f_{j\nu}(x+t) = e^{i\nu t} f_{j\nu}(x), \quad (\text{E.11})$$

with $J^- = \nu$. The Peter-Weyl expansion boils down to just the Fourier expansion of a function on \mathbb{R} . We denote this set $\{|\nu_L\rangle, \nu \in \mathbb{R}\}$, with coordinates space expansion:

$$\langle x | \nu_L \rangle = e^{i\nu x}. \quad (\text{E.12})$$

Likewise, the subgroup

$$\mathbf{h}_+ = \begin{pmatrix} 1 & t \\ 0 & 1 \end{pmatrix} = \exp itJ^+, \quad t \in \mathbb{R}, \quad (\text{E.13})$$

is diagonalized by $f_{j\nu}(x) = |x|^{2j} e^{i\frac{\nu}{x}}$ with eigenvalue $e^{i\nu t}$ and hence $J^+ = \nu$. The set $\{|\nu_R\rangle, \nu \in \mathbb{R}\}$ then has

$$\langle x | \nu_R \rangle = |x|^{2j} e^{i\frac{\nu}{x}}, \quad (\text{E.14})$$

$$\langle \nu_R | x \rangle = |x|^{-2j-2} e^{-i\frac{\nu}{x}}. \quad (\text{E.15})$$

The second relation can be seen as the definition of the bra $\langle \nu_R |$, and can be derived by finding the adjoint operator \mathbf{S}^\dagger of the operator \mathbf{S} introduced below.

These eigenfunctions also follow from directly diagonalizing \hat{J}^+ or \hat{J}^- from (E.9). Moreover, using the relations (E.9) it is easily seen that the $\nu = 0$ state in either basis, satisfying $\hat{J}^+ |0_R\rangle = 0$ and $\hat{J}^- |0_L\rangle = 0$, can be seen as a lowest/ highest weight state in the elliptic basis, with $i\hat{J}^0 |0_{R/L}\rangle = \mp j |0_{R/L}\rangle$. Both sets of states are complete bases, and their eigenfunctions are related by applying the matrix

$$\mathbf{S} = \begin{pmatrix} 0 & 1 \\ -1 & 0 \end{pmatrix} \quad (\text{E.16})$$

in coordinate space as

$$\mathbf{S} \cdot \langle x | \nu_R \rangle = \langle x | -\nu_L \rangle, \quad (\text{E.17})$$

or using the equivalence relation:

$$\mathbf{S}^{-1} \mathbf{h}_+ \mathbf{S} = \mathbf{h}_-. \quad (\text{E.18})$$

In particular, one has

$$\langle \nu_L | \lambda_R \rangle = \langle -\nu_R | \mathbf{S} | \lambda_R \rangle. \quad (\text{E.19})$$

E.2 Constrained $\text{SL}(2, \mathbb{R})$ basis

A matrix element of a representation is defined as the overlap:

$$R_{ab}(g) \equiv \langle ja | g | jb \rangle. \quad (\text{E.20})$$

Imposing the constraints $J^- = \sqrt{\mu}$, $\bar{J}^+ = \sqrt{\mu}$ on (E.20) shows that for the Schwarzian states, the a -index needs to be an eigenvalue of J^- and the b -index needs to be an eigenvalue of J^+ . The more general representation matrix elements to consider in the main text are hence matrix elements in a *mixed parabolic basis*, where the ket is taken from (E.12) and the bra from (E.14):

$$J^+ |\lambda_R\rangle = \lambda |\lambda_R\rangle, \quad (\text{E.21})$$

$$\langle \nu_L | J^- = \langle \nu_L | \nu. \quad (\text{E.22})$$

The Schwarzian states are embedded in this as $\lambda = \nu = \sqrt{\mu}$. This unconventional basis comes with potential subtleties, but for the computation of the relevant $3j$ - and $6j$ -symbols, these are immaterial due to the following fact. The equality (E.19) allows us to prove an important property of the representation integrals in the main text:

$$\int dg \langle \lambda_L | g | \lambda'_R \rangle \langle \mu_L | g | \mu'_R \rangle \langle \nu_L | g | \nu'_R \rangle = \int dg \langle \lambda_R | g | \lambda'_R \rangle \langle \mu_R | g | \mu'_R \rangle \langle \nu_R | g | \nu'_R \rangle, \quad (\text{E.23})$$

where in the last line we used the shift $\mathbf{S} \cdot g \rightarrow g$ and the invariance of the Haar measure under this shift. This demonstrates that this computation reduces to the standard representation integrals in the parabolic basis $\{|\nu_R\rangle\}$. The fact that the constrained $\text{SL}(2, \mathbb{R})$ system is described in a mixed basis, is hence irrelevant for the computation of these integrals. This is pivotal, as it is precisely these integrals that give $3j$ -symbols and ultimately $6j$ -symbols of $\text{SL}(2, \mathbb{R})$.

The overlap between basisvectors from both sets is given by

$$\begin{aligned} \langle \nu_L | \lambda_R \rangle &= \int_{-\infty}^{+\infty} dx |x|^{2j} e^{-i\nu x} e^{i\frac{\lambda}{x}} \\ &= 2 \int_0^{+\infty} dx |x|^{2j} e^{-i\nu x} e^{i\frac{\lambda}{x}} \\ &= 4 \left(-\frac{\lambda}{\nu} \right)^{j+1/2} K_{2j+1} \left(2\sqrt{\nu\lambda} \right). \end{aligned} \quad (\text{E.24})$$

Instructive examples to compute are

$$\langle \nu_L | \exp(itJ^+) | \lambda_R \rangle = \exp(it\lambda) \langle \nu_L | \lambda_R \rangle, \quad (\text{E.25})$$

$$\langle \nu_L | \exp(itJ^-) | \lambda_R \rangle = \exp(it\nu) \langle \nu_L | \lambda_R \rangle, \quad (\text{E.26})$$

where the second relation can be readily obtained by using (E.5) to act on the left with J^- .

The Gauss decomposition of a generic $\text{SL}(2, \mathbb{R})$ matrix is given by:

$$g = \begin{pmatrix} 1 & 0 \\ \gamma_L & 1 \end{pmatrix} \begin{pmatrix} e^{-\phi} & 0 \\ 0 & e^{\phi} \end{pmatrix} \begin{pmatrix} 1 & \gamma_R \\ 0 & 1 \end{pmatrix}, \quad (\text{E.27})$$

with corresponding metric

$$ds^2 = \frac{1}{2} \text{Tr} [(g^{-1}dg)^2] = d\phi^2 + e^{-2\phi} d\gamma_L d\gamma_R. \quad (\text{E.28})$$

Relevant matrix elements are then found by using (E.25), (E.26), the integral (E.24) and the composition rule (E.4):

$$R_{j,\nu\lambda}(g) \equiv \langle \nu_L | g(\phi, \gamma_L, \gamma_R) | \lambda_R \rangle = 2 \left(-\frac{\lambda}{\nu} \right)^{j+1/2} e^\phi K_{2j+1}(2\sqrt{\nu\lambda}e^\phi) e^{i\nu\gamma_L + i\lambda\gamma_R}. \quad (\text{E.29})$$

One readily checks that the matrix element of the inverse g^{-1} has the property:

$$R_{j,\lambda\nu}(g^{-1}) \equiv \langle \lambda_R | g^{-1} | \nu_L \rangle = \overline{\langle \nu_L | g | \lambda_R \rangle}, \quad (\text{E.30})$$

demonstrating that the representation is unitary, as will be required as they represent physical wavefunctions of the BF model. The grand orthogonality theorem holds:

$$\int dg R_{j,\nu\lambda}(g) R_{j,\lambda'\nu'}(g^{-1}) = \frac{1}{\rho(j)} \int dg \langle g | j\nu\lambda \rangle \langle j'\lambda'\nu' | g \rangle = \frac{1}{\rho(j)} \delta(j-j') \delta(\nu-\nu') \delta(\lambda-\lambda'), \quad (\text{E.31})$$

due to the orthogonality of the plane waves, and the MacDonald-functions (4.14). From this expression, the Plancherel measure $\rho(j)$ can be distilled. Applying the Liouville constraints, the interesting matrix elements are

$$R_{j,\sqrt{\mu}\sqrt{\mu}} = \langle \sqrt{\mu}_L | g(\phi, \gamma_L, \gamma_R) | \sqrt{\mu}_R \rangle = 2 (-)^{j+1/2} e^\phi K_{2j+1}(2\sqrt{\mu}e^\phi) e^{i\sqrt{\mu}(\gamma_L + \gamma_R)}. \quad (\text{E.32})$$

Matrix elements in the mixed parabolic basis do not give unity when $\phi = \gamma_L = \gamma_R = 0$. In other bases (such as the elliptic one discussed recently in [83]), this fixes the normalization of the matrix element, from which the Plancherel measure can be derived in the end. Here the normalization of the matrix element is fixed by the *normalized* basis vectors $|\nu_L\rangle$ and $|\nu_R\rangle$. The analogue of the unit group element is played by setting $g = \mathbf{S}^{-1}$, which in Gauss coordinates (E.27) can be written as the locus:

$$\phi \rightarrow +\infty, \quad \gamma_L = e^\phi, \quad \gamma_R = -e^\phi. \quad (\text{E.33})$$

One can readily derive an addition theorem for two matrix elements (E.29) in the mixed parabolic basis. For simplicity we focus on only the ϕ -dependence.

$$\begin{aligned} & \int d\nu' d\lambda' \langle \nu_L | g(\phi_1) | \lambda'_R \rangle \langle \lambda'_R | \nu'_L \rangle \langle \nu'_L | g(\phi_2) | \lambda_R \rangle \\ &= \int d\nu' d\lambda' \int dx dy dz |x|^{2j} |y|^{-2j-2} |z|^{2j} e^{-i\nu x} e^{i\frac{\lambda'}{x} e^{2\phi_1}} e^{-i\frac{\lambda'}{y}} e^{i\nu' y} e^{-i\nu' z} e^{i\frac{\lambda}{z} e^{2\phi_2}} \\ &= \int dx |x|^{2j} e^{-i\nu x} e^{i\frac{\lambda}{x} e^{2\phi_1 + 2\phi_2}} \\ &= \langle \nu_L | g(\phi_1 + \phi_2) | \lambda_R \rangle. \end{aligned} \quad (\text{E.34})$$

In coordinate space:

$$\begin{aligned} & \int d\nu' d\lambda' K_{2j+1}(2\sqrt{\nu\lambda'}e^{\phi_1}) K_{2j+1}(2\sqrt{\lambda'\nu'}) K_{2j+1}(2\sqrt{\nu'\lambda}e^{\phi_2}) \\ &= 2 (-)^{j+1/2} K_{2j+1}(2\sqrt{\nu\lambda}e^{\phi_1 + \phi_2}). \end{aligned} \quad (\text{E.35})$$

E.3 From the $\text{SL}(2, \mathbb{R})$ Casimir to the minisuperspace Liouville Hamiltonian

To the Gauss parametrization (E.27), one can associate the left- and right-regular realization of the algebra:

$$\begin{aligned} i\hat{\mathcal{D}}_L^- &= \partial_{\gamma_L}, & i\hat{\mathcal{D}}_R^- &= -\gamma_R^2 \partial_{\gamma_R} - \gamma_R \partial_\phi + e^{2\phi} \partial_{\gamma_L}, \\ i\hat{\mathcal{D}}_L^0 &= -2\gamma_L \partial_{\gamma_L} - \partial_\phi, & i\hat{\mathcal{D}}_R^0 &= -2\gamma_R \partial_{\gamma_R} - \partial_\phi, \\ i\hat{\mathcal{D}}_L^+ &= -\gamma_L^2 \partial_{\gamma_L} - \gamma_L \partial_\phi + e^{2\phi} \partial_{\gamma_R}, & i\hat{\mathcal{D}}_R^+ &= \partial_{\gamma_R}, \end{aligned} \quad (\text{E.36})$$

with Casimir operator, computed in either realization:

$$\hat{\mathcal{C}} = \left(\hat{\mathcal{D}}^0\right)^2 + \frac{1}{2} \left(\hat{\mathcal{D}}^+ \hat{\mathcal{D}}^- + \hat{\mathcal{D}}^- \hat{\mathcal{D}}^+\right) = -\frac{1}{4} \partial_\phi^2 + \frac{1}{2} \partial_\phi - e^{2\phi} \partial_{\gamma_L} \partial_{\gamma_R}. \quad (\text{E.37})$$

The $\text{SL}(2, \mathbb{R})$ Casimir eigenvalue problem

$$\hat{\mathcal{C}} \chi(\phi, \gamma_L, \gamma_R) = \left(\frac{1}{4} + s^2\right) \chi(\phi, \gamma_L, \gamma_R), \quad (\text{E.38})$$

complemented with the Liouville constraints $i\partial_{\gamma_L} = i\partial_{\gamma_R} = \sqrt{\mu}$, and upon extracting a factor e^ϕ from the eigenfunction as $\chi = e^\phi \psi$, simplifies to

$$\left(-\frac{1}{4} \partial_\phi^2 + \mu e^{2\phi}\right) \psi_s(\phi) = s^2 \psi_s(\phi), \quad (\text{E.39})$$

which is a 1d Liouville equation, with normalizable solution:

$$\psi_s(\phi) = K_{2is}(2\sqrt{\mu}e^\phi). \quad (\text{E.40})$$

The potential and its solution are sketched below (Figure 16). This reduces the $\text{SL}(2, \mathbb{R})$

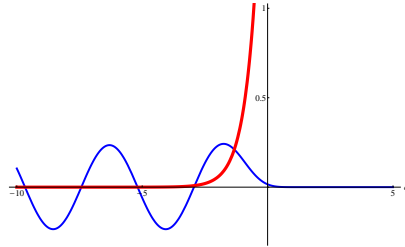


Figure 16. 1d Liouville potential (red), with normalizable solution $\psi_s(\phi)$ superimposed (blue).

system to the Liouville model, where only the continuous sector survives as normalizable solutions. The discrete modes are found by inverting the sign of the exponential potential (opposite sign for \mathcal{J}^- and $\tilde{\mathcal{J}}^+$), and are hence indeed absent in the constrained theory. This construction can be compared to that given in section 4.1 in 2d.

E.4 $6j$ -symbol

When proceeding with the $6j$ -computation, one should not resort to the above addition theorem (E.34). Instead, one separates the lines using

$$\int d\lambda \langle \nu_L | g_1 | \lambda_R \rangle \langle \lambda_R | g_2 | \mu_R \rangle. \quad (\text{E.41})$$

The channel λ is integrated over, and hence the intermediate matrix elements such as $\langle \nu_L | g_1 | \lambda_R \rangle$ do *not* satisfy the Liouville constraints (E.21)(E.22). This means that this step is only possible due to our knowledge on how to embed Liouville / Schwarzian within an $\text{SL}(2, \mathbb{R})$ system. This is only required when calculating crossed Wilson lines (OTO-correlators) and resonates with the fact that also in [23] we need to go outside the strict 1d theory in order to have a natural understanding on how folded time contours work. Drawing L labels in red, and R labels in black, this corresponds to the following picture:



(E.42)

Half of the matrix elements are now fully in the parabolic basis $|\nu_R\rangle$ (the right half of the picture), and lead to $3j$ -symbols as usual. For the other half (the red-black left half), we resort to the identity (E.23) to transform these into the standard parabolic basis as well. The $6j$ -symbol computation then follows the standard approach, with the only difference the continuous labels m that are integrated over (with flat measure):

$$\begin{Bmatrix} R_B & R_1 & R_4 \\ R_A & R_3 & R_2 \end{Bmatrix} = \int dm_i dm_A dm_B \begin{pmatrix} R_1 & R_2 & R_A \\ m_1 & m_2 & m_A \end{pmatrix} \begin{pmatrix} R_2 & R_3 & R_B \\ m_2 & m_3 & m_B \end{pmatrix} \begin{pmatrix} R_3 & R_4 & R_A \\ m_3 & m_4 & m_A \end{pmatrix} \begin{pmatrix} R_4 & R_1 & R_B \\ m_4 & m_1 & m_B \end{pmatrix}. \quad (\text{E.43})$$

F Representation Theory of $\text{SL}(n, \mathbb{R})$ in the Parabolic Basis

The generalization to the Hamiltonian reduction of $\text{SL}(n, \mathbb{R})$ is known, and it is useful to present some of the details. We follow [39, 78] and focus on $\text{SL}(3, \mathbb{R})$. We will make some comments of the general case as we go along. The eight traceless $\text{SL}(3, \mathbb{R})$ generators can be written:

$$\begin{aligned} H_1 &= \begin{pmatrix} i & 0 & 0 \\ 0 & -i & 0 \\ 0 & 0 & 0 \end{pmatrix}, & H_2 &= \begin{pmatrix} 0 & 0 & 0 \\ 0 & i & 0 \\ 0 & 0 & -i \end{pmatrix}, \\ J_1^+ &= \begin{pmatrix} 0 & -i & 0 \\ 0 & 0 & 0 \\ 0 & 0 & 0 \end{pmatrix}, & J_2^+ &= \begin{pmatrix} 0 & 0 & 0 \\ 0 & 0 & -i \\ 0 & 0 & 0 \end{pmatrix}, & J_{12}^+ &= \begin{pmatrix} 0 & 0 & -i \\ 0 & 0 & 0 \\ 0 & 0 & 0 \end{pmatrix}, \\ J_1^- &= \begin{pmatrix} 0 & 0 & 0 \\ i & 0 & 0 \\ 0 & 0 & 0 \end{pmatrix}, & J_2^- &= \begin{pmatrix} 0 & 0 & 0 \\ 0 & 0 & 0 \\ 0 & i & 0 \end{pmatrix}, & J_{12}^- &= \begin{pmatrix} 0 & 0 & 0 \\ 0 & 0 & 0 \\ i & 0 & 0 \end{pmatrix}. \end{aligned} \quad (\text{F.1})$$

The generators with multiple indices are associated to non-simple roots, and the indexation refers to how they are created from commutators. All off-diagonal matrices generate

parabolic subgroups of $\mathrm{SL}(n, \mathbb{R})$ as

$$\exp\{itJ_1^+\} = \begin{pmatrix} 1 & t & 0 \\ 0 & 1 & 0 \\ 0 & 0 & 1 \end{pmatrix}, \quad \text{etc.} \quad (\text{F.2})$$

The Hamiltonian reduction is obtained by fixing all generators of simple roots $J_i^+ = \sqrt{\mu_i}$, and all remaining ones (in this case only J_{12}) to zero:

$$J_i^+ = \sqrt{\mu_i}, \quad J_{ij\dots} = 0. \quad (\text{F.3})$$

The Gauss decomposition can be generalized to this case, as

$$g = e^{i\gamma_L^{ij\dots} J_{ij\dots}^-} \mathbf{h} e^{i\gamma_R^{ij\dots} J_{ij\dots}^+} \quad (\text{F.4})$$

with $\mathbf{h} = \prod_i \exp\{i\phi_i H_i\}$ the Cartan group element, in this case $\mathbf{h} = \exp\{i\phi_1 H_1\} \exp\{i\phi_2 H_2\}$, for $N - 1$ fields ϕ_i , combined in the vector ϕ . These will become the Toda CFT fields.

States in a representation are labeled with the eigenvalue of the Cartan subgroup (in this case H_1 and H_2) on the highest weight state. We denote the labels as j_i , combined in the vector \mathbf{j} .

As for the $n = 2$ case, two different bases are constructed. The R -basis diagonalizes the J_i^+ matrices, the L -basis diagonalizes the J_i^- matrices. The overlap between both bases gives the analogue of (E.24), and represents a solution to the $\mathrm{SL}(n, \mathbb{R})$ Toda minisuperspace eigenvalue problem, just like the mixed parabolic matrix elements of $\mathrm{SL}(2, \mathbb{R})$ satisfy the 1d Liouville equation. The simplest way to obtain these wavefunctions is to diagonalize the operators J_i^+ or J_i^- in the Borel-Weil realization [78, 84], analogous to (E.9). For $n = 3$, the coordinate space wavefunctions are given by:

$$\langle x_1, x_2, x_{12} | \sqrt{\mu_1}_L \sqrt{\mu_2}_L \rangle = e^{i\sqrt{\mu_1}x_1 + i\sqrt{\mu_2}x_2}, \quad (\text{F.5})$$

$$\langle \sqrt{\mu_1}_R \sqrt{\mu_2}_R | x_1, x_2, x_{12} \rangle = (x_{12} - x_1 x_2)^{-2j_2 - 2} x_{12}^{-2j_1 - 2} e^{-i\sqrt{\mu_2} \frac{x_1}{x_{12}}} e^{-i\sqrt{\mu_1} \frac{x_2}{x_1 x_2 - x_{12}}}, \quad (\text{F.6})$$

and the overlap $\langle \sqrt{\mu_1}_L \sqrt{\mu_2}_L | \sqrt{\mu_1}_R \sqrt{\mu_2}_R \rangle$ can be computed in principle. In practice, only the $n = 2$ case allows a direct evaluation of the integrals. The general matrix element of interest is then given by

$$R_{\mathbf{j}, \sqrt{\mu_i} \sqrt{\mu_i}}(\phi) \equiv \langle \sqrt{\mu_i}_L | \mathbf{h} | \sqrt{\mu_i}_R \rangle, \quad (\text{F.7})$$

and is called the Whittaker function. These representation matrices are to be inserted in the computation in the main text to produce $3j$ - and eventually $6j$ -symbols. As earlier, the group integrals over the $\gamma_L^{ij\dots}$ and $\gamma_R^{ij\dots}$ variables reduce to delta-functions, and the computation boils down in essence to a Toda calculation:

$$\int d\phi R_{\mathbf{j}_1, \sqrt{\mu_i} \sqrt{\mu_i}}(\phi) V_1(\phi) R_{\mathbf{j}_2, \sqrt{\mu_i} \sqrt{\mu_i}}(\phi) = \left(\begin{array}{ccc} \mathbf{j}_1 & 1 & \mathbf{j}_2 \\ \sqrt{\mu_i} & \mathbf{0} & \sqrt{\mu_i} \end{array} \right)^2, \quad (\text{F.8})$$

where $V_1 = e^{\langle \mathbf{1}, \phi \rangle}$ is the Toda vertex operator. This in principle solves the problem. It remains to be seen whether these expressions can be made more explicit.

References

- [1] A. Kitaev, Talk given at the Fundamental Physics Prize Symposium, [Nov. 10, 2014](#); A. Kitaev, KITP seminar, [Feb. 12, 2015](#); “A simple model of quantum holography,” talks at KITP, [April 7, 2015](#) and [May 27, 2015](#).
- [2] S. Sachdev and J.-w. Ye, “Gapless spin fluid ground state in a random, quantum Heisenberg magnet,” *Phys. Rev. Lett.* **70** (1993) 3339, [arXiv:cond-mat/9212030 \[cond-mat\]](#).
- [3] J. Polchinski and V. Rosenhaus, “The Spectrum in the Sachdev-Ye-Kitaev Model,” *JHEP* **1604**, 001 (2016) [arXiv:1601.06768 \[hep-th\]](#).
- [4] A. Jevicki, K. Suzuki and J. Yoon, “Bi-Local Holography in the SYK Model,” *JHEP* **1607**, 007 (2016) [arXiv:1603.06246 \[hep-th\]](#).
- [5] J. Maldacena and D. Stanford, “Remarks on the Sachdev-Ye-Kitaev model,” *Phys. Rev. D* **94**, no. 10, 106002 (2016) [arXiv:1604.07818 \[hep-th\]](#).
- [6] A. Jevicki and K. Suzuki, “Bi-Local Holography in the SYK Model: Perturbations,” *JHEP* **1611**, 046 (2016) [arXiv:1608.07567 \[hep-th\]](#).
- [7] G. Turiaci and H. Verlinde, “Towards a 2d QFT Analog of the SYK Model,” *JHEP* **1710** (2017) 167 [arXiv:1701.00528 \[hep-th\]](#).
- [8] D. J. Gross and V. Rosenhaus, “The Bulk Dual of SYK: Cubic Couplings,” *JHEP* **1705** (2017) 092 [arXiv:1702.08016 \[hep-th\]](#).
- [9] D. J. Gross and V. Rosenhaus, “All point correlation functions in SYK,” *JHEP* **1712** (2017) 148 [arXiv:1710.08113 \[hep-th\]](#).
- [10] S. R. Das, A. Jevicki and K. Suzuki, “Three Dimensional View of the SYK/AdS Duality,” *JHEP* **1709** (2017) 017 [arXiv:1704.07208 \[hep-th\]](#).
- [11] S. R. Das, A. Ghosh, A. Jevicki and K. Suzuki, “Space-Time in the SYK Model,” [arXiv:1712.02725 \[hep-th\]](#).
- [12] A. Kitaev and S. J. Suh, “The soft mode in the Sachdev-Ye-Kitaev model and its gravity dual,” [arXiv:1711.08467 \[hep-th\]](#).
- [13] R. Jackiw, “Lower Dimensional Gravity,” *Nucl. Phys. B* **252**, 343 (1985)
- [14] C. Teitelboim, “Gravitation and Hamiltonian Structure in Two Space-Time Dimensions,” *Phys. Lett.* **126B** (1983) 41.
- [15] R. Jackiw, “Gauge theories for gravity on a line,” *Theor. Math. Phys.* **92** (1992) 979 [*Teor. Mat. Fiz.* **92** (1992) 404] [arXiv:hep-th/9206093 \[hep-th\]](#).
- [16] A. Almheiri and J. Polchinski, “Models of AdS₂ backreaction and holography,” *JHEP* **1511**, 014 (2015) [arXiv:1402.6334 \[hep-th\]](#).
- [17] K. Jensen, “Chaos in AdS₂ Holography,” *Phys. Rev. Lett.* **117** (2016) no.11, 111601 [arXiv:1605.06098 \[hep-th\]](#).
- [18] J. Maldacena, D. Stanford and Z. Yang, “Conformal symmetry and its breaking in two dimensional Nearly Anti-de-Sitter space,” *PTEP* **2016**, no. 12, 12C104 (2016) [arXiv:1606.01857 \[hep-th\]](#).
- [19] J. Engelsoy, T. G. Mertens and H. Verlinde, “An investigation of AdS₂ backreaction and holography,” *JHEP* **1607**, 139 (2016) [arXiv:1606.03438 \[hep-th\]](#).

- [20] M. Cvetič and I. Papadimitriou, “AdS₂ holographic dictionary,” JHEP **1612**, 008 (2016) Erratum: [JHEP **1701**, 120 (2017)] [arXiv:1608.07018 \[hep-th\]](#).
- [21] G. Mandal, P. Nayak and S. R. Wadia, “Coadjoint orbit action of Virasoro group and two-dimensional quantum gravity dual to SYK/tensor models,” JHEP **1711** (2017) 046 [arXiv:1702.04266 \[hep-th\]](#).
- [22] P. Nayak, A. Shukla, R. M. Soni, S. P. Trivedi and V. Vishal, “On the Dynamics of Near-Extremal Black Holes,” [\[arXiv:1802.09547 \[hep-th\]\]](#).
- [23] T. G. Mertens, G. J. Turiaci and H. L. Verlinde, “Solving the Schwarzian via the Conformal Bootstrap,” JHEP **1708** (2017) 136 [arXiv:1705.08408 \[hep-th\]](#).
- [24] T. G. Mertens, “The Schwarzian Theory - Origins,” [arXiv:1801.09605 \[hep-th\]](#).
- [25] H. T. Lam, T. G. Mertens, G. J. Turiaci and H. Verlinde, “Shockwave S-matrix from Schwarzian Quantum Mechanics,” [arXiv:1804.09834 \[hep-th\]](#).
- [26] D. Bagrets, A. Altland and A. Kamenev, “Sachdev-Ye-Kitaev model as Liouville quantum mechanics,” Nucl. Phys. B **911** (2016) 191 [arXiv:1607.00694 \[cond-mat.str-el\]](#).
- [27] D. Bagrets, A. Altland and A. Kamenev, “Power-law out of time order correlation functions in the SYK model,” Nucl. Phys. B **921** (2017) 727 [arXiv:1702.08902 \[cond-mat.str-el\]](#).
- [28] J. Maldacena and Z. Yang, to appear.
- [29] D. Stanford and E. Witten, “Fermionic Localization of the Schwarzian Theory,” JHEP **1710** (2017) 008 [arXiv:1703.04612 \[hep-th\]](#).
- [30] R. A. Davison, W. Fu, A. Georges, Y. Gu, K. Jensen and S. Sachdev, “Thermoelectric transport in disordered metals without quasiparticles: The Sachdev-Ye-Kitaev models and holography,” Phys. Rev. B **95** (2017) no.15, 155131 [arXiv:1612.00849 \[cond-mat.str-el\]](#).
- [31] J. Yoon, “SYK Models and SYK-like Tensor Models with Global Symmetry,” JHEP **1710** (2017) 183 [arXiv:1707.01740 \[hep-th\]](#).
- [32] S. Choudhury, A. Dey, I. Halder, L. Janagal, S. Minwalla and R. Poojary, “Notes on Melonic $O(N)^{q-1}$ Tensor Models,” [arXiv:1707.09352 \[hep-th\]](#).
- [33] P. Narayan and J. Yoon, “Supersymmetric SYK Model with Global Symmetry,” [arXiv:1712.02647 \[hep-th\]](#).
- [34] A. Gaikwad, L. K. Joshi, G. Mandal and S. R. Wadia, “Holographic dual to charged SYK from 3D Gravity and Chern-Simons,” [arXiv:1802.07746 \[hep-th\]](#).
- [35] W. Fu, D. Gaiotto, J. Maldacena and S. Sachdev, “Supersymmetric Sachdev-Ye-Kitaev models,” Phys. Rev. D **95** (2017) no.2, 026009 Addendum: [Phys. Rev. D **95** (2017) no.6, 069904] [arXiv:1610.08917 \[hep-th\]](#).
- [36] H. A. Gonzalez, D. Grumiller and J. Salzer, “Towards a bulk description of higher spin SYK,” [arXiv:1802.01562 \[hep-th\]](#).
- [37] A. Blommaert, T. G. Mertens and H. Verschelde, “Edge Dynamics from the Path Integral: Maxwell and Yang-Mills,” [arXiv:1804.07585 \[hep-th\]](#).
- [38] E. Witten, “(2+1)-Dimensional Gravity as an Exactly Soluble System,” Nucl. Phys. B **311** (1988) 46.
- [39] M. Bershadsky and H. Ooguri, “Hidden SL(n) Symmetry in Conformal Field Theories,” Commun. Math. Phys. **126** (1989) 49.

- [40] H. L. Verlinde, “Conformal Field Theory, 2-*D* Quantum Gravity and Quantization of Teichmüller Space,” Nucl. Phys. B **337** (1990) 652.
- [41] E. Witten, “Quantum Field Theory and the Jones Polynomial,” Commun. Math. Phys. **121** (1989) 351.
- [42] S. Elitzur, G. W. Moore, A. Schwimmer and N. Seiberg, “Remarks on the Canonical Quantization of the Chern-Simons-Witten Theory,” Nucl. Phys. B **326** (1989) 108.
- [43] G. W. Moore and N. Seiberg, “Taming the Conformal Zoo,” Phys. Lett. B **220** (1989) 422.
- [44] L. Iliesiu, S. Pufu, Y. Wang, “To appear”
- [45] S. Cordes, G. W. Moore and S. Ramgoolam, “Lectures on 2-d Yang-Mills theory, equivariant cohomology and topological field theories,” Nucl. Phys. Proc. Suppl. **41** (1995) 184
[arXiv:9411210 \[hep-th\]](#).
- [46] E. Witten, “On quantum gauge theories in two-dimensions,” Commun. Math. Phys. **141** (1991) 153.
- [47] A. A. Migdal, “Recursion Equations in Gauge Theories,” Sov. Phys. JETP **42** (1975) 413 [Zh. Eksp. Teor. Fiz. **69** (1975) 810].
- [48] E. Witten, “Two-dimensional gauge theories revisited,” J. Geom. Phys. **9** (1992) 303
[arXiv:9204083 \[hep-th\]](#).
- [49] W. Donnelly and G. Wong, “Entanglement branes in a two-dimensional string theory,” JHEP **1709** (2017) 097 [arXiv:1610.01719 \[hep-th\]](#).
- [50] M. S. Marinov and M. V. Terentev, “Dynamics On The Group Manifolds And Path Integral,” Fortsch. Phys. **27** (1979) 511.
- [51] M. f. Chu and P. Goddard, “Quantization of a particle moving on a group manifold,” Phys. Lett. B **337** (1994) 285 [arXiv:9407116 \[hep-th\]](#).
- [52] D. J. Gross and W. Taylor, “Twists and Wilson loops in the string theory of two-dimensional QCD,” Nucl. Phys. B **403** (1993) 395 [arXiv:9303046 \[hep-th\]](#).
- [53] A. Giveon, D. Kutasov and N. Seiberg, “Comments on string theory on AdS(3),” Adv. Theor. Math. Phys. **2** (1998) 733 [arXiv:9806194 \[hep-th\]](#).
- [54] J. Teschner, “The Minisuperspace limit of the $sl(2,C) / SU(2)$ WZNW model,” Nucl. Phys. B **546** (1999) 369 [arXiv:9712258 \[hep-th\]](#).
- [55] J. Teschner, “Operator product expansion and factorization in the $H+(3)$ WZNW model,” Nucl. Phys. B **571** (2000) 555 [arXiv:9906215 \[hep-th\]](#).
- [56] J. M. Maldacena and H. Ooguri, “Strings in AdS(3) and $SL(2,R)$ WZW model 1.: The Spectrum,” J. Math. Phys. **42** (2001) 2929 [arXiv:0001053 \[hep-th\]](#).
- [57] R. Dijkgraaf, H. L. Verlinde and E. P. Verlinde, “String propagation in a black hole geometry,” Nucl. Phys. B **371** (1992) 269.
- [58] S. Carlip, “Dynamics of asymptotic diffeomorphisms in (2+1)-dimensional gravity,” Class. Quant. Grav. **22** (2005) 3055 [arXiv:0501033 \[gr-qc\]](#).
- [59] G. Compere, L. Donnay, P. H. Lambert and W. Schulgin, “Liouville theory beyond the cosmological horizon,” JHEP **1503** (2015) 158 [arXiv:1411.7873 \[hep-th\]](#).

- [60] O. Coussaert, M. Henneaux and P. van Driel, “The Asymptotic dynamics of three-dimensional Einstein gravity with a negative cosmological constant,” *Class. Quant. Grav.* **12** (1995) 2961 [arXiv:9506019 \[gr-qc\]](#).
- [61] A. Alekseev and S. L. Shatashvili, “Path Integral Quantization of the Coadjoint Orbits of the Virasoro Group and 2D Gravity,” *Nucl. Phys. B* **323** (1989) 719.
- [62] A. Alekseev and S. L. Shatashvili, “From geometric quantization to conformal field theory,” *Commun. Math. Phys.* **128** (1990) 197.
- [63] Y. Hikida and V. Schomerus, “ $H+(3)$ WZNW model from Liouville field theory,” *JHEP* **0710** (2007) 064 [[arXiv:0706.1030 \[hep-th\]](#)].
- [64] N. Y. Vilenkin and A. U. Klimyk, “Representation of Lie Groups and Special Functions: Volume 1,” Kluwer Academic Publishers, 1991.
- [65] C. B. Thorn, “Liouville perturbation theory,” *Phys. Rev. D* **66** (2002) 027702 [arXiv:0204142 \[hep-th\]](#).
- [66] E. Braaten, T. Curtright, G. Ghandour and C. B. Thorn, “A Class of Conformally Invariant Quantum Field Theories,” *Phys. Lett.* **125B** (1983) 301.
- [67] E. Braaten, T. Curtright, G. Ghandour and C. B. Thorn, “Nonperturbative Weak Coupling Analysis of the Quantum Liouville Field Theory,” *Annals Phys.* **153** (1984) 147.
- [68] N. Seiberg, “Notes on quantum Liouville theory and quantum gravity,” *Prog. Theor. Phys. Suppl.* **102**, 319 (1990).
- [69] A. Gervois and H. Navelet, “Some Integrals Involving Three Modified Bessel Functions. 2.,” *J. Math. Phys.* **27** (1986) 688.
- [70] A. Gervois and H. Navelet, “Some Integrals Involving Three Modified Bessel Functions. 1.,” *J. Math. Phys.* **27** (1986) 682.
- [71] D. Basu and K. B. Wolf, “The Clebsch-gordan Coefficients of the Three-dimensional Lorentz Algebra in the Parabolic Basis,” *J. Math. Phys.* **24** (1983) 478.
- [72] I. S. Gradshteyn and I. M. Ryzhik, “Tables of integrals, sums, series and derivatives,” *Izd. Fizmatgiz* (1963).
- [73] W. Groenevelt, “The Wilson function transform,” [arXiv:0306424 \[math.CA\]](#).
- [74] W. Groenevelt, “Wilson function transforms related to Racah coefficients,” [arXiv:math/0501511 \[math.CA\]](#).
- [75] A. L. Fitzpatrick, J. Kaplan, D. Li and J. Wang, “Exact Virasoro Blocks from Wilson Lines and Background-Independent Operators,” *JHEP* **1707** (2017) 092 [arXiv:1612.063858 \[hep-th\]](#).
- [76] Y. Hikida and V. Schomerus, “Structure constants of the $OSP(1-2)$ WZNW model,” *JHEP* **0712** (2007) 100 [arXiv:0711.0338 \[hep-th\]](#).
- [77] M. R. Douglas, I. R. Klebanov, D. Kutasov, J. M. Maldacena, E. J. Martinec and N. Seiberg, “A New hat for the $c=1$ matrix model,” In *Shifman, M. (ed.) et al.: From fields to strings, vol. 3* 1758-1827 [arXiv:0307195 \[hep-th\]](#).
- [78] A. Gerasimov, S. Kharchev, A. Marshakov, A. Mironov, A. Morozov and M. Olshanetsky, “Liouville type models in group theory framework. 1. Finite dimensional algebras,” *Int. J. Mod. Phys. A* **12** (1997) 2523 [arXiv:9601161 \[hep-th\]](#).

- [79] M. Besken, A. Hegde, E. Hijano and P. Kraus, “Holographic conformal blocks from interacting Wilson lines,” JHEP **1608** (2016) 099 [arXiv:1603.07317 \[hep-th\]](#).
- [80] M. Guica, “Bulk fields from the boundary OPE,” [arXiv:1610.08952 \[hep-th\]](#).
- [81] G. Barnich, H. A. Gonzalez and P. Salgado-Rebolledo, “Geometric actions for three-dimensional gravity,” Class. Quant. Grav. **35** (2018) no.1, 014003 [arXiv:1707.08887 \[hep-th\]](#).
- [82] F. Falceto and K. Gawedzki, “Lattice Wess-Zumino-Witten model and quantum groups,” J. Geom. Phys. **11**, 251 (1993) [[hep-th/9209076](#)].
- [83] A. Kitaev, “Notes on $\widetilde{\text{SL}}(2, \mathbb{R})$ representations,” [arXiv:1711.08169 \[hep-th\]](#).
- [84] A. Chervov, “Raising operators for the Whittaker wave functions of the Toda chain and intertwining operators,” [arXiv:math/9905005 \[hep-th\]](#).